Agricultural Water Management 334 (2026) 110675

Contents lists available at ScienceDirect

Agricultural Water Management

journal homepage: www.elsevier.com/locate/agwat

Opportunities for bioenergy crops to support transitions from irrigated agriculture and conserve the U.S. High Plains Aquifer

Karthik Ramaswamy [a,b,*], Nazli Uludere Aragon [c], Tyler J. Lark [a,b,d,*]

[a] Center for Sustainability and the Global Environment, Nelson Institute for Environmental Studies, University of Wisconsin-Madison, Madison, WI 53726, USA
[b] DOE Great Lakes Bioenergy Research Center, University of Wisconsin-Madison, Madison, WI 53726, USA
[c] The Numerical Terradynamic Simulation Group, University of Montana, Missoula, MT 59812, USA
[d] Department of Plant, Soil, and Microbial Sciences, Michigan State University, East Lansing, MI 48824, USA

ARTICLE INFO

Keywords:
Groundwater depletion
Cropping system adaptation
Hydro-economic modeling
Bioenergy feedstocks
Land use transitions
irrigation economics

ABSTRACT

This study investigates potential economic and groundwater driven transitions from irrigated maize production—the dominant irrigated cropping system in the High Plains Aquifer (HPA) region—to alternative crops such as sorghum and switchgrass, two common bioenergy feedstocks. Unsustainable groundwater extraction in the U.S. High Plains presents critical challenges including reduced irrigation capacities, diminished crop yields, lower land values, and escalating energy costs. Using a spatially explicit optimization framework combined with comprehensive economic and hydrogeological data, we evaluate optimal land-use strategies and irrigation system investments over a 30-year planning period. Results indicate significant regional variability in the future economic viability of irrigated agriculture, driven by differences in aquifer recharge rates, groundwater availability, and market conditions. Nebraska and parts of northern Texas can sustain irrigated maize profitability due to relatively favorable groundwater conditions and lower land rents, respectively. In contrast, many portions of Kansas and southern Texas are more likely to transition to dryland agriculture within two decades. Colorado and New Mexico show potential for significant adoption of switchgrass production as an alternative biomass-based energy crop. Overall, over the 30-year horizon, our model implies that approximately 23% of currently irrigated maize area across the HPA region may transition to dryland farming under business-as-usual conditions. This transition is complemented by a threefold increase in non-irrigated sorghum production, from 0.20 to 0.77 Mt yr^{-1}, indicating that groundwater-driven shifts in agricultural production may support a larger regional base for bioenergy feedstocks. The study also reveals opportunities for producers to optimize economic returns and biomass production potential.

1. Introduction

The agricultural sector faces mounting pressure from groundwater depletion, especially in regions that have historically depended on it for irrigation. With irrigation increasingly constrained by water availability, it is essential to identify sustainable alternatives that reduce water use while limiting the impacts on farm profitability. Research that investigates alternative cropping systems, optimized irrigation practices, and informed policy interventions is crucial for ensuring the long-term viability of agriculture in these regions and safeguarding the economic well-being of communities reliant on these vital water resources (Araya et al., 2019).

This challenge is particularly acute in the U.S. High Plains, where the Ogallala Aquifer, one of the world's largest freshwater reserves, has supported decades of irrigated agriculture. Technological advances following World War II, including high-capacity wells and center pivot irrigation systems, led to widespread irrigation expansion (Hornbeck and Keskin, 2014). While these innovations enhanced productivity, they also accelerated the depletion of the Ogallala Aquifer, a largely non-renewable resource in many parts of the region. With rates of natural recharge often far below withdrawal, large sections of the central and southern High Plains now face severe declines in groundwater levels (Deines et al., 2020; Hornbeck and Keskin, 2014; Scanlon et al., 2012).

These hydrological trends have significant economic and ecological

* Correspondence to: Center for Sustainability and the Global Environment, Nelson Institute for Environmental Studies, 1710 University Ave, Madison, WI 53705, USA

E-mail addresses: ramaswk@okstate.edu (K. Ramaswamy), larktyle@msu.edu (T.J. Lark).

https://doi.org/10.1016/j.agwat.2026.110675
Received 14 October 2025; Received in revised form 4 July 2026; Accepted 27 July 2026
Available online 5 August 2026

implications. Groundwater depletion has reduced well capacities, driven up energy costs for pumping, and lowered land values (Alley et al., 1999; Perez-Quesada et al., 2024; Sampson et al., 2019). In turn, agricultural producers are responding with various adaptation strategies including transitioning to dryland crops, switching to less water-intensive crops such as sorghum or wheat, converting land to pasture, or temporarily retiring fields through programs like the Conservation Reserve Program (Deines et al., 2020; Rao and Yang, 2010; Roberts and Lubowski, 2007; Wallander et al., 2013). In more severe cases, land has been permanently withdrawn from production altogether. These adaptive responses are grounded in observable long-term shifts in groundwater availability. For instance, McGuire and Strauch (2024) reported changes in groundwater well levels from the 1950s to 2019, ranging from a rise of 26.21 m (86 ft) in Nebraska to a decline of 80.77 m (265 ft) in Texas. The state-level weighted average change was estimated at −0.12 m (−0.4 ft) for Nebraska and −13.44 m (−44.1 ft) for Texas, revealing stark regional contrasts. These divergences illustrate uneven patterns of aquifer depletion across the High Plains and the need for locally tuned strategies for resource management.

Yet, the High Plains Aquifer (HPA) region remains central to U.S. agriculture, both in terms of its contribution to national grain output and its role in supporting the livestock industry. The eight states overlying the HPA—Colorado, Kansas, Nebraska, New Mexico, Oklahoma, South Dakota, Texas, and Wyoming—comprise nearly 40% of U.S. agricultural land, and about 32% of croplands (USDA National Agricultural Statisitcs Service, 2022). Notably, we estimate that about 40% of the cultivated area in the High Plains region relies on irrigation from the Ogallala aquifer (Xie et al., 2021). Among the main crops grown in the region (by area)—wheat, hay, maize, soybeans, and to a lesser extent cotton—maize emerges as the crop that has been most consistently cultivated under irrigation (USDA National Agricultural Statisitcs Service, 2024a).

To help mitigate water sustainability concerns, crops like switchgrass (*Panicum viragatum* L.) and biomass sorghum (*Sorghum bicolor (L.) Moench*) offer less water-intensive alternatives to irrigated maize (*Zea mays* L.) in the region. These crops have high biomass potential and are relatively drought tolerant. Switchgrass, a native perennial, is well suited to marginal and degraded lands and requires fewer inputs, making it ideal for sustainable energy production without competing with prime cropland (Abraha et al., 2016; Blanco-Canqui, 2016; Hamilton et al., 2015). Sorghum, meanwhile, offers familiarity to producers, a shorter growing season, and competitive returns, particularly under declining well capacity (Cui et al., 2018; Ramaswamy, 2016; Warren et al., 2015).

Water sustainability is also a challenge for biofuel production, particularly when feedstocks are grown in heavily irrigated areas dependent upon nonrenewable groundwater resources (Chowdhury et al., 2025; Fingerman et al., 2010). Irrigated maize grown in the region contributes substantially to the nation's biofuel supply, and Nebraska is the second largest ethanol producing state. Thus, substituting irrigated maize with less water-intensive alternatives could also reduce the water footprint of supplied fuels, which currently consists of more than 80% maize-based ethanol (U.S. Energy Information Administration, 2024; USDA Economic Research Service, 2023).

We evaluate the long-term economic viability of transitioning from irrigated maize to alternative, less water-intensive crops that could also be utilized as bioenergy feedstocks under local groundwater constraints. Using an optimization framework that integrates spatially variable hydrological conditions and market dynamics, we estimate the economically rational potential for biomass sorghum and switchgrass to replace currently irrigated maize areas in the HPA. We also model dryland maize as the leading competing dryland crop to more realistically capture overall transition dynamics. The results reveal where and under what economic conditions these crops can be viable alternatives to irrigated maize.

2. Materials and methods

2.1. Approach

To assess and quantify the transitions from irrigated maize cultivation and the associated potential for bioenergy feedstock production across the HPA, we developed a spatially explicit optimization model. This model combines agronomic variables with hydrological ones related to irrigated fields' saturated thickness, hydraulic conductivity, and specific yield to assess the aquifer's potential to maintain irrigated agriculture, and the feasibility of transitioning to rainfed bioenergy feedstock cultivation when irrigated agriculture becomes unsustainable. Our model permits contraction of irrigation (i.e., irrigated fields may transition to dryland production or alternative crops) but does not allow expansion of irrigation into previously non-irrigated fields. By holding the irrigated land base constant at its observed extent, we isolate groundwater impacts associated with crop substitution decisions within the existing irrigated footprint.

Our approach, illustrated in Fig. 1, comprises these key steps:

1. Data and Preprocessing: Utilizing existing modeled data on aquifer and well characteristics to extrapolate current aquifer conditions in the study area.
2. Constructing an economic analysis to estimate the net returns under alternative irrigated (maize and sorghum) and non-irrigated (maize, sorghum and switchgrass) agricultural systems using an enterprise budget approach.
3. Determining the optimal irrigated and non-irrigated crop choices across the HPA, subject to groundwater constraints, using a 30-year mixed integer linear programming (MILP) model.

2.2. County level data

The HPA spans parts of eight states—Colorado, Kansas, Nebraska, New Mexico, Oklahoma, South Dakota, Texas, and Wyoming. This study builds upon the work of Ramaswamy (2024), which focused on groundwater-crop dynamics in five representative counties overlying the HPA. Expanding the spatial scope, the present analysis includes 180 counties across the HPA, while excluding peripheral counties with total areas under 100 km^2 and/or without irrigated land to maintain analytical relevance. County-level crop yield data (2000–2018) were sourced from the National Agricultural Statistics Service (NASS) QuickStats database of the US Department of Agriculture (USDA) for maize and sorghum (USDA–NASS, 2024b). Because county-year observations are not balanced across all states and years, some county-year pairs are not surveyed or are withheld, therefore we substitute agricultural district-level yields when available and otherwise use state-level yields for the corresponding irrigation status. These substitutions preserve the irrigated versus dryland distinction while ensuring complete coverage for model calibration.

For switchgrass, county-level average yields were derived using spatially explicit rainfed perennial grass productivity simulations based on PRISM climate data (Daly et al., 2018). These gridded yield estimates were aggregated to the county level and reflect average dryland switchgrass productivity under typical climate conditions to provide a consistent, regionally appropriate benchmark for modeling biomass potential in non-irrigated systems.

State average marketing prices and representative irrigated and dryland crop yields used for model calibration are reported in Appendix Table A.1 (USDA–NASS, 2024c). Maize and sorghum dominate irrigated cropland across the HPA, accounting for the majority of irrigated cropland in most states and therefore representing the primary drivers of groundwater extraction in the region. Dryland maize, dryland sorghum, and switchgrass constitute the principal observed non-irrigated systems and define the feasible transition pathways evaluated in the model. Appendix Table A.2 reports the major irrigated and non-irrigated crop

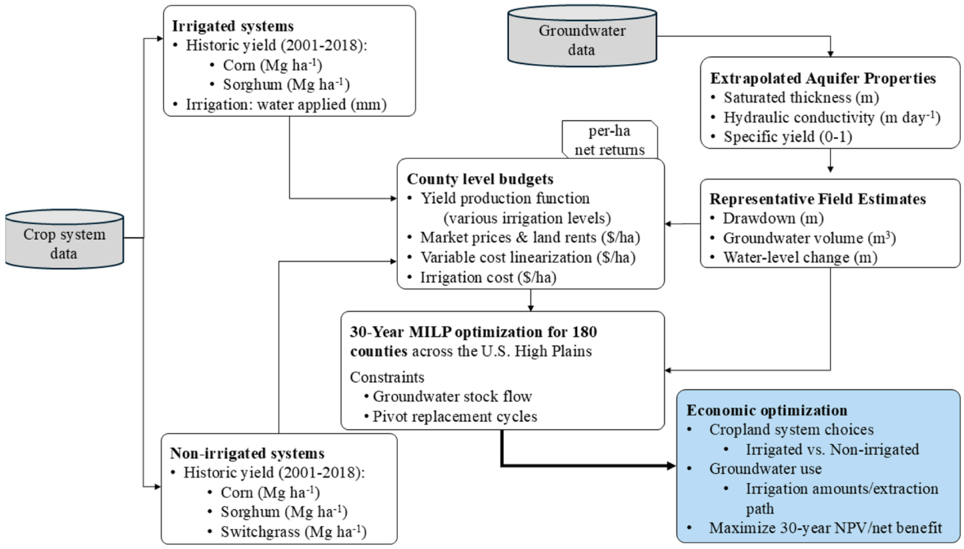

Fig. 1. Modeling approach and data integration. Multi-source data integration for optimizing agricultural systems, crop budgets, and aquifer dynamics. Assumptions are for a representative farm and groundwater availability.

categories across the HPA study region to place the modeled systems in the context of the broader baseline crop mix. Wheat is widespread in the HPA, particularly under dryland production, but it is not included as a modeled transition crop because its winter production calendar, seasonal water-use profile, and rotational role differ from the summer crop systems evaluated here. Wheat may also be followed by double-cropped summer crops in some parts of the High Plains, including soybean, sorghum, sunflower, and summer annual forages, but this practice depends strongly on wheat harvest timing, residual soil moisture, and the length of the remaining growing season. Incorporating wheat would therefore require a separate crop-calendar and rotation framework beyond the scope of the present analysis (Kansas State University Department of Agronomy, 2026).

Land rental rates were also obtained from NASS, and maize and sorghum prices (2018–2023) were collected from the USDA Agricultural Marketing Service. Direct production costs, including labor, insurance, fertilizer, seed, repairs, and interest were estimated using cost parameters from Kansas State University extension enterprise budgets (Kansas State University, 2024). Groundwater characteristics were derived from hydrogeologic parameters including saturated thickness and specific yield from McGuire et al. (2012), and permeability from Gleeson et al. (2014). Recent water level changes (2009–2019) were incorporated to refine estimates of saturated thickness over time. LANID irrigated field maps (2009–2017) from Xie et al. (2021) were used to spatially identify and mask actively irrigated croplands within each county, allowing groundwater storage and pumping estimates to be constrained to areas under irrigation. Each of these spatially refined data layers was subsequently aggregated to the county level to estimate total groundwater availability, potential pumping rates, and associated irrigation costs, which informed the characterization of representative irrigation cropping operations. County-level crop production parameters used in the optimization model, including irrigated yields, irrigation requirements, and production costs, are reported in Supplement S1.

2.3. *Farm and irrigated crop system characteristics*

We define a representative 48.6-ha (120-acre) center-pivot irrigated field drawing from a groundwater well with a 31.5 L s^{-1} pumping capacity as a standardized engineering unit for modeling purposes (Fig. 2). This "typical" system is not intended to represent uniform conditions across all counties. Rather, it serves as a tractable baseline configuration that allows for consistent simulation of irrigation decisions and

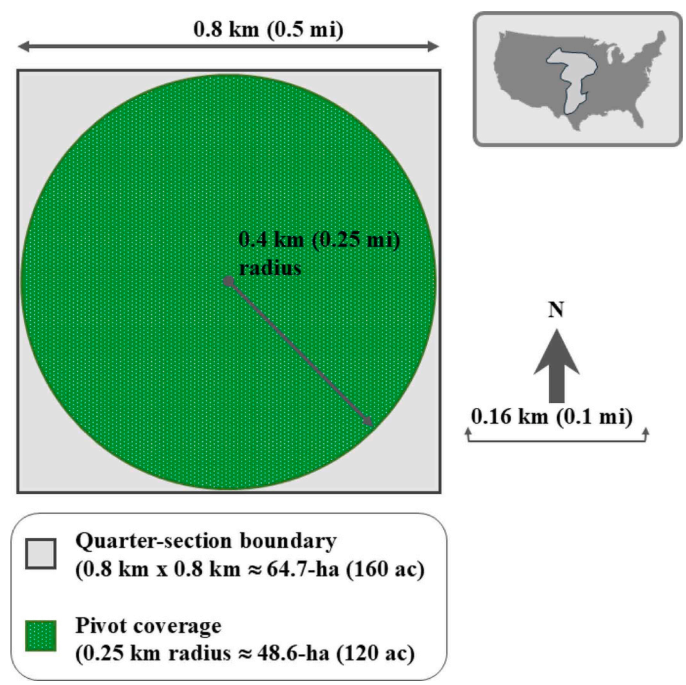

Fig. 2. Illustrates a typical farm field in the High Plains Aquifer region, showcasing a center pivot irrigation system on a 48.6-ha field within a 64.7-ha quarter section.

groundwater extraction across the study region. While the engineering configuration is fixed, its effective irrigation capacity, pumping cost, and yield response are determined by county-specific hydrogeologic parameters (e.g., saturated thickness, hydraulic conductivity, recharge) and crop productivity. Thus, the representative pivot operates under different economic and hydrologic constraints in each county, allowing spatial heterogeneity to emerge endogenously in the optimization results.

Field studies in the HPA indicate that net irrigation applications on the order of 457–559 mm (18–22 in.) are typically sufficient to sustain irrigated maize, with variations arising from growing season length and planting and harvest dates (Klocke et al., 2011; Kranz et al., 2010; Trout and DeJonge, 2017). In this study, we focus explicitly on net irrigated water applied, rather than total crop water requirements, and do not model precipitation separately. Instead, county-level observed yields implicitly reflect historical climatic conditions, including precipitation variability.

Using an assumed center pivot efficiency of 75% and application rates between 25.4 and 31.8 mm (1–1.25 in) per cycle, prior studies indicate that a well capacity of 31.5 L s^{-1} can supply sufficient net irrigation to support irrigated maize over a typical irrigation period of 60–120 days (New and Fipps, 2000). We adopt a 90-day irrigation period as a representative operating assumption for maize (our baseline irrigated crop) and irrigated sorghum; however, realized irrigation feasibility and groundwater impacts vary across the study region based on hydrogeologic and yield conditions. County-level irrigation requirements are estimated numerically by inverting yield response functions that relate crop yield to net irrigation applications using observed county-average yields as calibrated targets. This approach allows irrigation demand to vary spatially across counties while remaining consistent with observed production outcomes.

To model baseline irrigation water use from groundwater resources (i.e. drawdown), we needed to estimate minimum saturated thickness per well. For wells operating at capacities of 6.3, 12.6, 18.9, 25.2, and 31.5 L s^{-1} (100, 200, 300, 400, and 500 GPM), this was calculated using a 90-day cone of depression, applying Cooper and Jacob (1946) and Theis (1935) equations. Given the heterogeneous aquifer properties and varying well depths, the saturated thickness was stratified into five layers, each representing minimum thickness requirements for different pumping capacities (Ramaswamy, 2016). This stratification enhances accuracy in assessing drawdown effects and extraction costs. Well interference effects were found to be negligible at distances greater than 0.4 km (0.25-mi), meaning that the drawdown caused by one well does not materially impact the performance of neighboring wells beyond this separation distance. This threshold was used to assume operational independence among wells in the modeling framework.

Groundwater availability also depends critically on specific yield, which represents the fraction of aquifer storage that can be drained under gravity. Here, it is calculated as the product of land area, specific yield, and saturated thickness (Schloss et al., 2000). Specific yield/porosity values were obtained from spatially explicit USGS hydrogeologic datasets rather than assumed uniformly across the study region (McGuire et al., 2012). Our study assumes groundwater availability beneath a 64.7-ha land unit, of which 48.6-ha are irrigated. This reflects the standard footprint of a center-pivot irrigation system, which typically irrigates a circular area covering approximately 75% of a quarter section (Dieter et al., 2018; Lamm et al., 2015). The remaining area includes infrastructure or non-irrigated buffer zones. Importantly, hydrogeologic inputs (saturated thickness, specific yield, permeability) and observed county-level yields are spatially explicit, ensuring that model outcomes differ across the study region even though the engineering configuration of the representative pivot system is standardized. To approximate county-wide dynamics, we scale this representative field structure to reflect average conditions, recognizing that irrigated area generally comprises about 40% of total cropland across the High Plains (USDA National Agricultural Statistics Service, 2022).

We initialized hydrogeologic conditions using USGS 2009 spatial dataset of saturated thickness and water-level change since predevelopment as the baseline (McGuire et al., 2012). We then time-updated these conditions to 2017 using USGS biannual (2009–2017) water-level change grids to produce a 2017 saturated thickness surface (McGuire, 2013, 2014, 2017, McGuire, Strauch, 2022; McGuire and Strauch, 2024). To align with actively irrigated lands, we masked the updated saturated thickness using LANID for 2017 from Xie et al. (2021) and extended the computations through 2024 using average (2009–2017) water-level change to estimate the effective saturated thickness. County-level metrics were then calculated using zonal statistics, yielding irrigated-area-weighted averages of saturated thickness and water level changes (to determine the declining or recharging zones) for each county (Figs. 3a-3b).

Hydraulic parameterization combined (i) specific yield/porosity from USGS products (McGuire et al., 2012), and (ii) permeability/hydraulic conductivity from the GHYMPS database (Gleeson et al., 2014). Using these parameters with the irrigated area weighted effective saturated thickness, we classified sustainable well capacities for 6.3, 12.6, …, 31.5 L s^{-1} with approximately 9 m (~30 ft) as a safety zone at the bottom of the aquifer. To be consistent with the prior work, we excluded pixels with saturated thickness < 9.1 m as operationally unsustainable for center-pivot irrigation (Deines et al., 2020; Haacker et al., 2016; Hecox et al., 2002).

Pumping costs are estimated using the Nebraska Pumping Plant Performance Criteria (NPC), which relates pumping energy requirements to total depth and system efficiency. County-level total well depth was defined as the vertical distance from land surface to the pumping water level, incorporating static water level and drawdown. As groundwater levels decline, total well-depth increases, resulting in greater pumping lift and higher energy requirements per unit of water pumped. Energy use was calculated as a function of pumping lift and efficiency following NPC guidelines and multiplied by prevailing energy prices to estimate irrigation pumping costs. Thus, irrigation costs in the model vary dynamically with groundwater conditions. They increase as saturated thickness declines depth to water rises. County-level groundwater parameters used in the hydro-economic model, including aquifer properties and pumping cost estimates, are provided in Supplement S2.

2.4. Economic analysis

Our economic analysis consists of two major steps: (1) developing crop budgets for each agricultural system for 180 HPA counties for irrigated maize, irrigated sorghum, non-irrigated maize, non-irrigated sorghum and switchgrass (resulting in 900 budgets), and (2) constructing county-specific 30-year MILP models to determine the optimal cropland system choices, groundwater use, and net present value (NPV) for a representative field. The production value of the irrigated lands is determined by finding the optimal extraction path (annual withdrawal amount from the aquifer) of limited groundwater for irrigation of maize and grain sorghum based on the concept of "User Cost," which represents the potential future profits lost due to current resource use (Dasgupta and Heal, 1979; Hotelling, 1931; Stoecker et al., 1985; Vaux, 2011). Our overall aim is to maximize total profits over the life of the aquifer based on the theoretical framework in Appendix B.

We developed representative crop budgets for irrigated (maize and sorghum) and non-irrigated (maize, sorghum, and switchgrass) production systems as follows:

1. To estimate irrigated maize and sorghum yields under different well capacities, we began with county-level yield averages from USDA NASS, which we assumed to reflect production under relatively unconstrained irrigation conditions approximated here as 31.5 L s^{-1} well capacity. This means the crops receive sufficient water throughout the growing season.
2. Next, following Lamm et al. (2007), we determine the yield response for irrigated maize and sorghum to well capacities from 6.3 L s^{-1} to 25.2 L s^{-1} in increments of 6.3 L s^{-1} based on possible water application using pivot irrigation frequency during growing season, which is a key factor in our economic analysis. Then using the relative yield response identified the irrigation to be applied for well capacities 6.3, 12.6, …, 31.5 L s^{-1} was estimated following Klocke et al. (2011) for maize and Klocke et al. (2012) for sorghum, focusing on western Kansas. Well capacity influences crop yields because higher capacities allow for more irrigation, potentially leading to higher yields, especially during periods of peak water demand (Irmak, 2015; Klocke et al., 2012, 2011; Rudnick et al., 2019; Trout and DeJonge, 2017).

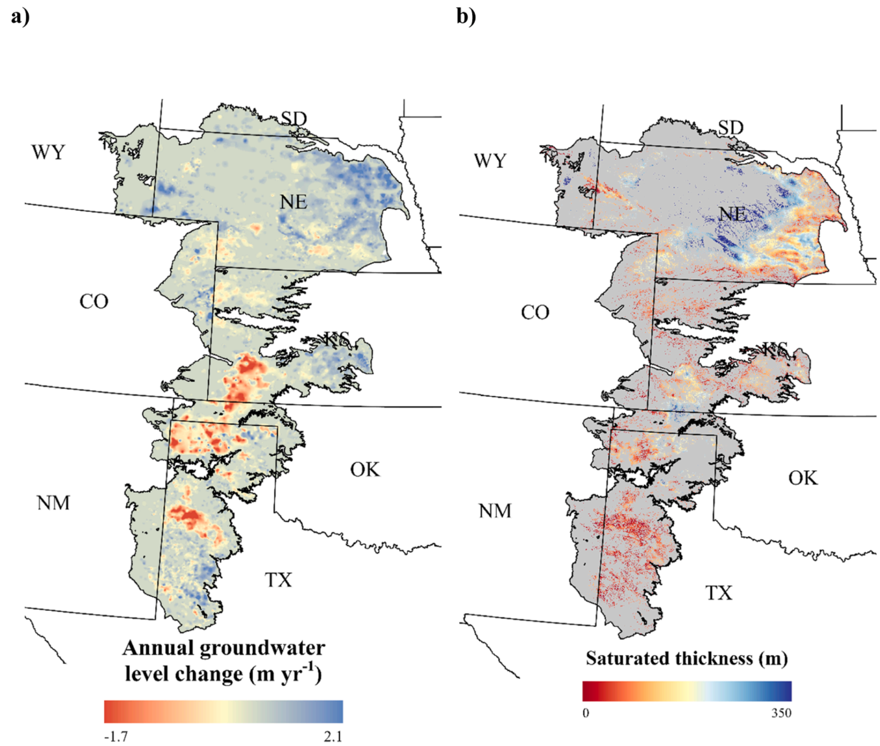

Fig. 3. Spatial variation in groundwater conditions across the U.S. High Plains Aquifer. a) mean rate of groundwater level changes from 2009 to 2024 based on (McGuire and Strauch, 2024), b) estimated aquifer thickness within irrigated areas as of 2024, representing available groundwater storage used in this study.

3. The predicted yields were then used to estimate relative irrigation amounts using numerical methods (Abramowitz and Stegun, 1964). We used the same response function for all HPA counties due to the lack of recently available studies from other parts of the HPA.

Predicted irrigated yields could deviate from the observed responses due to differences in soil (e.g., texture and water holding capacity), climate (e.g., precipitation and evapotranspiration demand), or management practices between counties in western Kansas and other parts of the HPA. Applying a single crop yield and well capacity response function across the HPA represent a simplification. By using county-level observed yields to calibrate the fully irrigated production level, we preserve spatial heterogeneity in baseline productivity. The uniform response function therefore governs relative yield reductions under constrained well capacity rather than absolute yield levels. While this assumption may bias the marginal response locally, it is a tractable and transparent approach in absence of consistent, region-wide empirical response functions. The predicted yields were then used to construct county-specific enterprise budgets for irrigated systems. Gross revenues were calculated using county-level yields combined with observed price data (2018–2023 averages), ensuring that spatial heterogeneity in productivity directly translates into spatial variation in revenues. We based production costs on Kansas State University extension enterprise budgets. We held fixed cost components constant across counties. We modeled variable costs (e.g., fertilizer, harvesting, crop insurance, and other input costs) as functions of spatially varying crop yields. This approach reflects economic heterogeneity in production systems across the HPA while maintaining a consistent cost structure, thereby allowing the analysis to isolate the effects of groundwater availability and well capacity constraints on profitability and cropping decisions.

We developed county-specific switchgrass enterprise budgets using average dry matter biomass yields (Mg ac^{-1}) for each HPA county, and include baling and hauling costs, which scale proportionally with biomass output. Establishment costs were amortized over a 10-year stand life, and fertilizer and other operating expenses were included based on extension recommendations (Brandes et al., 2018; Griffith et al., 2014).

Several key assumptions underpin the MILP portion of our economic analysis. First, our model uses a 30-year planning horizon to evaluate crop choices, irrigated and non-irrigated area, and biomass production. Next, consistent with other economic studies, we rely on the "single-cell aquifer" hydrological representation to model temporal allocation of the groundwater. While groundwater is a common pool resource in practice, the single-cell aquifer representation treats water availability as an exogenous stock constraint within each field unit. Simply put, the aquifer is assumed to be spatially homogeneous within the unit of analysis (48.6-ha field). Although aquifer properties, well depth and drawdown (cone of depression) that limits the extraction capacity can vary widely in space, this simplification is necessary because there is currently inadequate information to capture heterogeneity at the irrigated field level for modeling purposes (Bredehoeft and Young, 1970; Brozović et al., 2010; Gisser and Mercado, 1972; Wheeler et al., 2008).

The overall objective of the MILP is to maximize the NPV per field over the 30-year planning horizon. The objective function represents long-term profit maximization at the representative field level rather than coordinated aquifer-wide welfare optimization. Each representative field maximizes its own net present value subject to groundwater constraints, without internalizing spillovers to neighboring wells or counties. The model optimizes over crop selection, irrigation amount, and timing of pivot investment subject to constraints on water availability, land availability, and capital costs. Existing research often treats irrigation investment costs either solely as variable operating expense or as levelized costs that amortize capital expenditures over the system's expected life (Lamm et al., 2015; O'Brien et al., 1998). While this approach simplifies economic modeling per unit of land, it may obscure important real-world constraints. Financing primarily affects the timing of cash flow rather than the discrete nature of the adoption decision. Furthermore, explicit modeling of loan amortization would introduce additional financial structure beyond the scope of this study but would not alter the binary nature of the pivot adoption decision. In practice, irrigation systems typically require substantial upfront capital investment – costs that are indivisible or lumpy, and producers must commit the full investment before irrigating any portion of the land. This poses a critical barrier, especially where financing is limited or unavailable (Frisvold and Deva, 2012; Morris and Persons, 2019). By modeling irrigation investment as a discrete capital investment rather than a smoothly scalable cost, our framework better reflects adoption realities and the nonlinear nature of irrigation expansion decisions under capital constraints.

The MILP model considers a binary "go / no-go" decision representing the initial investment decision to establish irrigated production through center pivot irrigation systems at the outset of the planning horizon. This binary decision explicitly captures the strategic choice faced by landowners—whether to incur the fixed initial investment costs associated with pivot installation, thereby committing to subsequent years of irrigated cropping under increasing uncertainty of available groundwater resources, or foregoing irrigation investments altogether. It also differentiates between county-level irrigated fields that are viable under long-term groundwater constraints and those that are not.

In this analysis, the decision to install a pivot system happens at the beginning of the planning period. This methodological choice distinguishes long-term optimal investment strategies from economically suboptimal or unsustainable alternatives. For this analysis, all county-field units start with new pivot systems that are purchased at the outset of the project. The step-change in adoption timing is driven by the simplifying assumption that all pivots start at the same age (new) in year 1, leading to synchronized replacement decisions, distributing initial pivot ages would smooth this pattern. This assumption also facilitates a comparison of long-term economic benefits, crop management strategies, and water use efficiency, controlling for initial infrastructure conditions. It also simplifies economic calculations by avoiding the need to make assumptions about the remaining economic life for existing irrigation systems in the HPA, for which reliable data are lacking.

A typical center pivot system has a lifespan of approximately 15 years, which constrains the model to allow for a maximum of two full investment cycles over the 30-year simulation period. Sensitivity testing conducted outside the scope of this paper suggests that introducing additional investment cycles has little impact on the model's long-term outcome. This insensitivity is primarily due to the dominant role of structural constraints, namely limited groundwater availability, and declining marginal returns to crop productivity under irrigation, which exert greater influence on long-run economic decision-making than the specific timing or frequency of infrastructure renewal.

When it is time to replace the pivots in year 16, the model evaluates whether to invest in a new pivot system and continue irrigated production for an additional 15 years, or to transition to a dryland cropping system, depending on which option yields the highest net returns. The transition to dryland farming is modeled as a gradual process based on remaining groundwater – fields begin to reduce irrigated area as well capacity decline due to falling groundwater availability, eventually resulting in a full conversion to dryland crops when groundwater becomes insufficient to support continued irrigation investment.

The net present value is calculated using an annual discount rate of 7 %. The cost of replacing the center pivot is assumed to be US$75,000 (real terms) per field with a typical lifespan of 15 years (Lamm et al., 2015; Reynolds et al., 2020).

Let $t = 1, 2, \ldots, T$ index years (with $T = 30$), and let $i \in \mathbb{C}$ are index crop activities (irrigated maize, irrigated sorghum, non-irrigated maize, non-irrigated sorghum, and switchgrass). The model maximizes NPV of profits over the planning horizon:

$$\max \text{NPV} = \sum_{t=1}^{T} \frac{1}{(1+r)^{t-1}} [\pi_t - K z_t] \tag{1}$$

where r is the annual discount rate (0.07), K is the fixed cost of pivot purchase or replacement (US \$75,000), and $z_t \in \{0, 1\}$ is a binary indicator that equals 1 if a pivot investment occurs in year t. Pivots are allowed only at the beginning of each 15-year equipment cycle (years 1 and 16:

$$z_t = 0 \quad \forall t \quad \notin \quad \{1, \quad 16\}, z_{16} \le z_1 \tag{2}$$

To represent pivot availability, let $P_t \in \{0, 1\}$ indicate whether a pivot is operational in year t. Given a 15-year irrigation system life, pivot availability is:

$$P_t = z_1 \quad \forall t = 1, \ldots, \quad 15; P_t = z_{16} \quad \forall t = 16, \ldots, \quad 30 \tag{3}$$

Annual profit (π_t) in year t is defined as:

$$\pi_t = \sum_{i \in \mathbb{C}} [p_i Y_i(w_{i,t}) - VC_i(Y_i(w_{i,t}))] A_{i,t} - C_t^{pump}(Q_t, D_t) \tag{4}$$

where p_i is the output price, $Y_i(\bullet)$ denotes the crop specific yield response function to irrigation application (Mg ha^{-1}) evaluated at irrigation depth $w_{i,t}$ (mm), and $VC_i(\bullet)$ denotes non-pumping variable cost per hectare (US\$ ha^{-1}), $A_{i,t}$ is crop area (ha), $C_t^{pump}(Q_t, D_t)$ is pumping cost (US\$) as a function of annual groundwater withdrawal Q_t (m^3 yr^{-1}) and depth-to-water D_t (m). For non-irrigated crops, irrigation depth is set to $w_{i,t} = 0$ and the yield function reduces to dryland yield.

2.4.1. Land constraint and pivot feasibility

Total planted area cannot exceed the representative field size (48.6 ha):

$$\sum_{i \in \mathbb{C}} A_{i,t} \le 48.6 \forall t \tag{5}$$

Irrigated crop areas are feasible only when a pivot is operational. Let $\mathbb{C}_{irr} \subset \mathbb{C}$ denotes irrigated crops (irrigated maize or irrigated sorghum). Then:

$$\sum_{i \in \mathbb{C}_{irr}} A_{i,t} \le 48.6 \bullet P_t \forall t \tag{6}$$

2.4.2. Well capacity (annual pumping limit)

Well capacity is represented in discrete pumping-rate classes $k_t \in \{6.3, 12.6, 18.9, 25.2, 31.5\}$ L s^{-1}. The feasibility capacity class k_t is exogenously determined each year from simulated saturated thickness and is not a decision variable. Annual groundwater withdrawal is constrained by the feasible pumping rate over time and irrigation season length H days:

$$Q_t \le 0.001 \bullet k_t \bullet 86,400 \bullet H \forall t \tag{7}$$

where 0.001 converts liters to m^3, 86,400 converts seconds per day.

Linkage between pumping and irrigation (water accounting identity):

Annual groundwater withdrawal equals total irrigation applied across irrigated crops. With irrigation depth $w_{i,t}$ in mm and area $A_{i,t}$ in ha:

$$Q_t = \sum_{i \in \mathbb{C}_{irr}} (10 \bullet w_{i,t} \bullet A_{i,t}) \tag{8}$$

where the factor 10 converts mm-ha to m^3 (since 1 mm applied over 1 ha equals 10 m^3).

2.4.3. Groundwater stock dynamics (cell aquifer)

Groundwater availability is represented by using single-cell aquifer formulation in which groundwater storage evolves annually as:

$$S_{t+1} = S_t - Q_t + R_t \quad \forall t \tag{9}$$

where S_t is the groundwater stock at start of the year t (m^3), R_t is the annual recharge (m^3 yr^{-1}). Storage is bound below by an operational minimum corresponding to a 9-m saturated thickness buffer:

$$S_t \ge S_{\min}, S_{\min} = (48.6 \times 10,000) SY \times 9 \tag{10}$$

where SY is specific yield (unitless) and 48.6 × 10,000 converts the representative field area from hectares to m^2. This single cell representation assumes spatial homogeneity within the representative field and does not allow lateral groundwater movement between counties, implying recharge effects are localized at the modeled unit.

2.4.4. Notation summary

Indices: $t = 1, \ldots, T$ (years, $T = 30$); $i \in \mathbb{C}$ (crop activities); $\mathbb{C}_{irr} \subset \mathbb{C}$ (irrigated crops).

Decision variables: $A_{i,t}$ (area allocated to crop i in year t, ha); $w_{i,t}$ (irrigated depth applied to crop i in year t, mm); z_t (binary pivot investment decision); P_t (binary pivot availability indicator).

State variables: S_t (groundwater stock at start of year t, m^3).

Derived variables: Q_t (annual groundwater withdrawal, m^3); k_t (feasible well-capacity class, L s^{-1}).

Parameters: p_i (output price); $Y_i(\bullet)$ (yield response function); $V_i(\bullet)$ (variable cost per hectare); $C_t^{pump}(\bullet)$ (pumping cost function); R_t (recharge); r (discount rate); K (pivot investment cost); SY (specific yield); H (irrigation season length in days).

Unless explicitly noted otherwise, all results and reported outcomes represent the 30-year modeling period and are relative to the baseline of irrigated cropland area, which we assume to be under maize (or maize rotation) cultivation. Irrigation expansion beyond the observed irrigated footprint is not permitted. The land base is fixed at baseline conditions, allowing the model to isolate groundwater impacts associated with crop substitution and irrigation contraction.

3. Results

We assessed the baseline production system of conventional irrigated maize against alternative cropping systems of sorghum and switchgrass and identified the economic and hydrological conditions under which transitions among crop systems are optimal. Transitions away from irrigated agriculture occur once the marginal value of irrigated production no longer cover the associated input costs, including production, center-pivot sprinkler investment, and groundwater extraction. This outcome is contingent on three conditions: (i) reduced groundwater availability that limits investment for irrigated production, (ii) diminishing marginal productivity due to deficit water application to crops, and (iii) increases in water pumping costs. We first examine projected changes in groundwater across the Northern, Central, and Southern HPA units, and subsequently assess the implications for crop transitions, biomass production, and bioenergy feedstock potential. Detailed county-level annual optimization results over the 30-year simulation period are reported in Supplement S3.

3.1. Change in groundwater levels

The spatial variation in groundwater endowments and depletion pathways across the HPA shapes the timing and extent of irrigation transitions over time. Modeled aquifer volumes at the beginning and end of the simulation period reveal substantial differences across the Northern, Central, and Southern HPA units. Figs. 4a-4c illustrates the spatial variability in aquifer volumes per hectare across the High Plains at the beginning (Fig. 4a), at the reinvestment period (Fig. 4b), and at the conclusion of the 30-year simulation period (Fig. 4c). These differences reflect underlying heterogeneities in initial storage levels, extraction intensities, and local recharge dynamics, which together determine the path and direction of depletion.

Initially, aquifer volumes exhibit notable contrasts aligned with the major aquifer units. The Northern High Plains dominated by Nebraska and extending into South Dakota and Wyoming, contains the largest groundwater reserves (688.40 km^3), with Nebraska accounting for approximately 683.45 km^3 of initial storage. The Central High Plains, including Kansas and eastern Colorado, begins with moderate reserves (e.g., 90.14 km^3 in Kansas and 31.33 km^3 in Colorado), while the Southern High Plains, including Texas, Oklahoma and New Mexico, exhibits comparatively smaller initial storage volumes (e.g., 40.56 km^3 in Texas, 14.21 km^3 in Oklahoma, and 0.84 km^3 in New Mexico). By the conclusion of the simulation period, substantial groundwater depletion occurs throughout much of the aquifer. The Southern High Plains experiences the most pronounced depletions; for example, Texas retains only 41.1% (16.69 km^3) of its initial groundwater volume, whereas Oklahoma retains 69.3% (9.85 km^3), and New Mexico retains 58.6% (0.49 km^3), reflecting intensive groundwater extraction pressures and minimal recharge rates. The Northern High Plains demonstrates greater aquifer sustainability, with Nebraska maintaining about 77.8% (532.00 km^3) of its initial groundwater storage, and both South Dakota and Wyoming retaining more than 70% of their respective volumes by year 30. The Central High Plains exhibits intermediate outcomes, with Kansas and Colorado retaining approximately 50.4% (45.47 km^3) and 42.5% (13.31 km^3) of their initial volumes, respectively, highlighting regional variations in groundwater extraction and recharge dynamics.

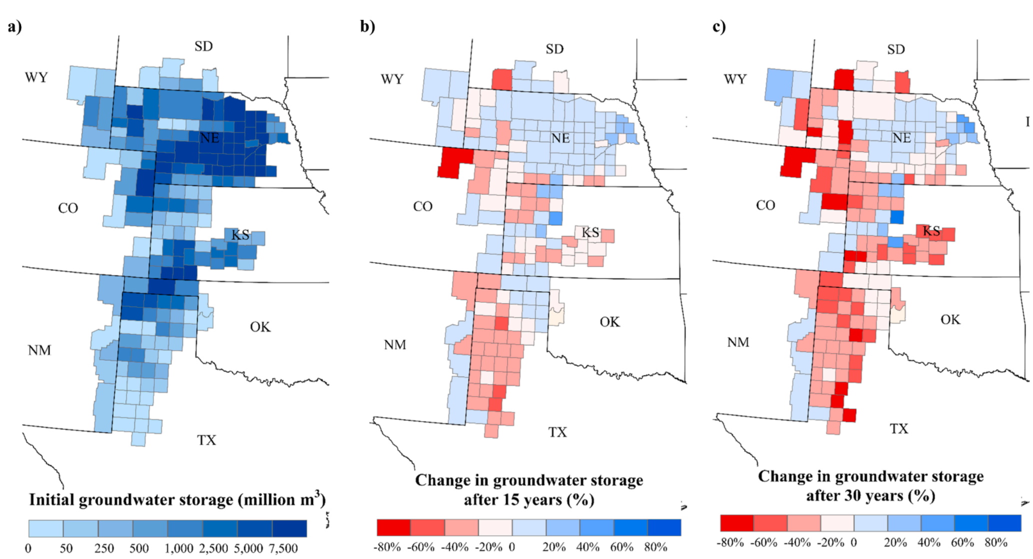

Fig. 4. Spatiotemporal dynamics of groundwater storage across the U.S. High Plains Aquifer during the 30-year simulation period. a) Initial aquifer storage volume (m^3) within irrigated maize area at the beginning of the simulation period, b) Relative change in storage after 15 years (%), normalized to initial volume, c) Relative change after 30 years (%), normalized to initial volume.

County-level groundwater storage dynamics over the simulation horizon are reported in Supplement S4.

3.2. Shifts to lower well capacities and transitions to dryland production

We find that 685,645 ha (1.69 million acres) of cropland transition from irrigated to dryland agricultural production in the U.S. HPA over the 30-year simulation period (Fig. 5 and Table 1 below). This includes acreage where it is already economical to be in dryland production (162,925 ha) under baseline conditions, as well as an additional 522 thousand hectares expected to shift in profitability. Overall, the dryland transition represents 23.1% of the currently irrigated maize area of 2.97 million hectares (7.33 million acres) in the region. The timing of dryland transitions and the corresponding remaining aquifer storage at the time of transition are mapped in Fig. 5a and Fig. 5b, respectively. Transitions occur earliest in the Southern High Plains and later in portions of the Northern High Plains. The distribution of irrigation well-capacity categories across counties and simulation years is reported in Supplement S5 and the timing of irrigated-to-dryland transitions across counties is reported in Supplement S6.

Fig. 6 presents the evolution of crop composition and remaining aquifer storage over the 30-year simulation period. Irrigated maize dominates cropland allocation during the early years but declines steadily as available groundwater decreases and extraction costs rise. At year 16, a shift in land allocation occurs due to pivot investment, resulting in transitions from irrigated maize to dryland maize and sorghum. By year 30, approximately 23.1% of cropland has transitioned to dryland systems. Aggregate cropland allocation by crop type over the simulation horizon is reported in Supplement S7.

The modeled crop shifts reflect a decline in well capacities. At the beginning of the simulation, 92% of irrigated area is supported by the highest capacity wells, and dryland cultivation for maize (and sorghum) is practiced in only 5.5% of the fields we modeled (Table 1). By the reinvestment point, the share of irrigated areas supported by the highest capacity wells decreases to 75.6%; this share declines further to 68.2% by year 30.

For the northern portion of the HPA (primarily Nebraska, South Dakota, and Wyoming), irrigation remains comparatively resilient over the 30-year horizon. For Nebraska, model results indicate that out of 1.88 million irrigated maize hectares, approximately 78.6% are projected to remain under irrigated production throughout the 30-year period. About 6% of this area is already economically favorable to transition to dryland production, based on marginal returns from initial pivot investment cost. At the time of pivot reinvestment, a further 14.4% of the irrigated maize area is expected to shift to dryland agricultural systems. Across Nebraska, most irrigated counties can maintain irrigation with high-capacity wells supported by approximately 579.96 million m^3 of groundwater stock and consistent recharge of 17.32 million m^3. Similarly, counties in South Dakota and Wyoming maintain high-capacity systems throughout the simulation period, reflecting lower irrigation intensity and more stable saturated thickness conditions.

In the central HPA (irrigated counties of Kansas and eastern Colorado) we observe a larger decline in acreage irrigated by high-capacity wells from 90.1% (685,233 ha) to 57.1%. Here, irrigation at lower-capacity wells and dryland production both expand from 7% to 21.5%. Over the course of the simulation period, Kansas shows a clear trajectory of groundwater depletion and corresponding adjustments in irrigation practices. Initially, more than 85% of the irrigated maize acreage in the state is supported by high-capacity wells. At pivot reinvestment time, the share of acreage supported by high-capacity wells has declined to 69.8%, while 5% of irrigated area is supplied by intermediate- and lower capacity wells, and the remaining 26% shifts to dryland production. By year 30, the irrigated acreage supported by

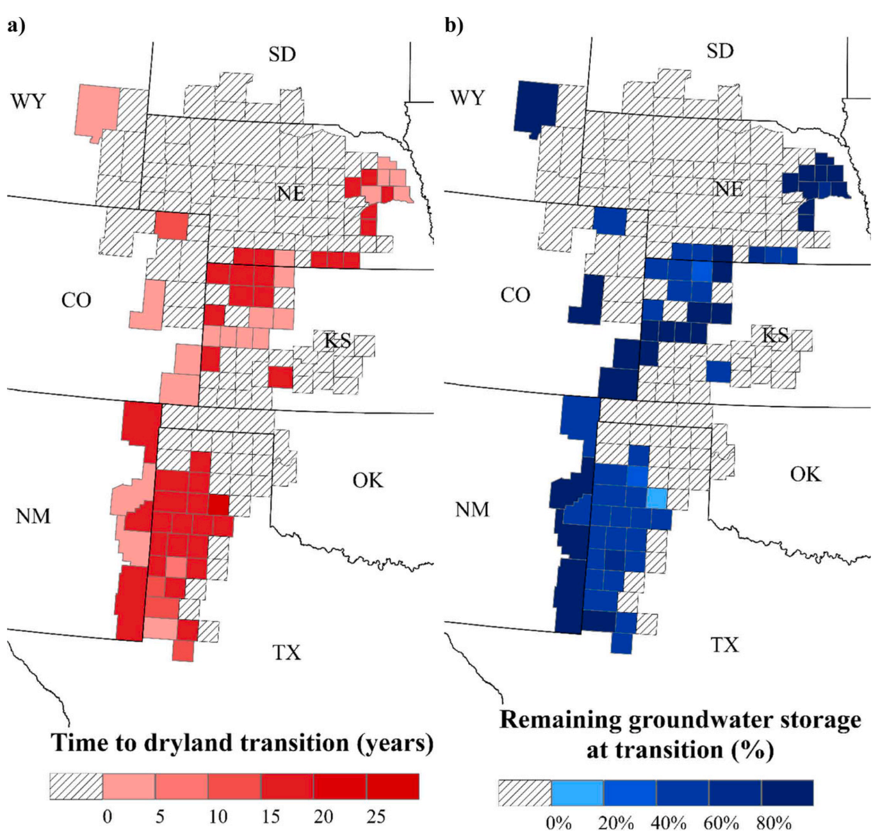

Fig. 5. Spatiotemporal transition from irrigated to dryland production across the U.S. High Plains Aquifer region, a) Number of years until irrigated maize production becomes economically or hydrologically infeasible, and b) Fraction of initial aquifer storage remaining at the time of transition. Cross-hatched counties denote no transition during the 30-year modeling period.

Table 1
Distribution of irrigated cropland by well-capacity class under baseline and year 30 conditions across the U.S. High Plains Aquifer (HPA).

		Baseline (%)				Year 30 (%)			
Region / State	Area (ha)	High	Intermediate	Low	Dryland	High	Intermediate	Low	Dryland
Northern High Plains									
NE	1,883,445	93.9	0.0	0.0	6.1	79.0	0.4	0.0	20.6
SD	3,306	100.0	0.0	0.0	0.0	99.9	0.0	0.1	0.0
WY	22,195	99.4	0.0	0.0	0.6	42.0	57.4	0.0	0.6
NHP total	1,908,947	94.0	0.0	0.0	6.0	78.6	1.1	0.0	20.4
Central High Plains									
KS	497,202	90.0	3.4	0.4	6.1	48.1	26.0	0.0	26.0
CO	188,031	90.3	1.3	0.0	8.4	80.9	9.5	0.2	9.5
CHP total	685,233	90.1	2.9	0.3	6.7	57.1	21.4	0.1	21.4
Southern High Plains									
TX	305,124	86.6	13.4	0.0	0.0	26.8	29.7	0.0	43.5
OK	50,126	100.0	0.0	0.0	0.0	100.0	0.0	0.0	0.0
NM	17,464	11.5	74.1	0.0	14.3	0.0	0.0	0.0	100.0
SHP total	372,714	84.8	14.5	0.0	0.7	35.3	24.4	0.0	40.3
HPA total	2,966,894	92.0	2.5	0.1	5.5	68.2	8.7	0.0	23.1

Note: High (31.5–25.2 L s^{-1}), intermediate (18.9–12.6 L s^{-1}), and low (6.3 L s^{-1}) denote well capacity classes corresponding to 500–400, 300–200, and 100 GPM, respectively. Percentages represent shares of total irrigated area by state. NHP stands for Northern High Plains, CHP for Central High Plains, and SHP for Southern High Plains. Area represents baseline irrigated cropland used in model calibration in hectares.

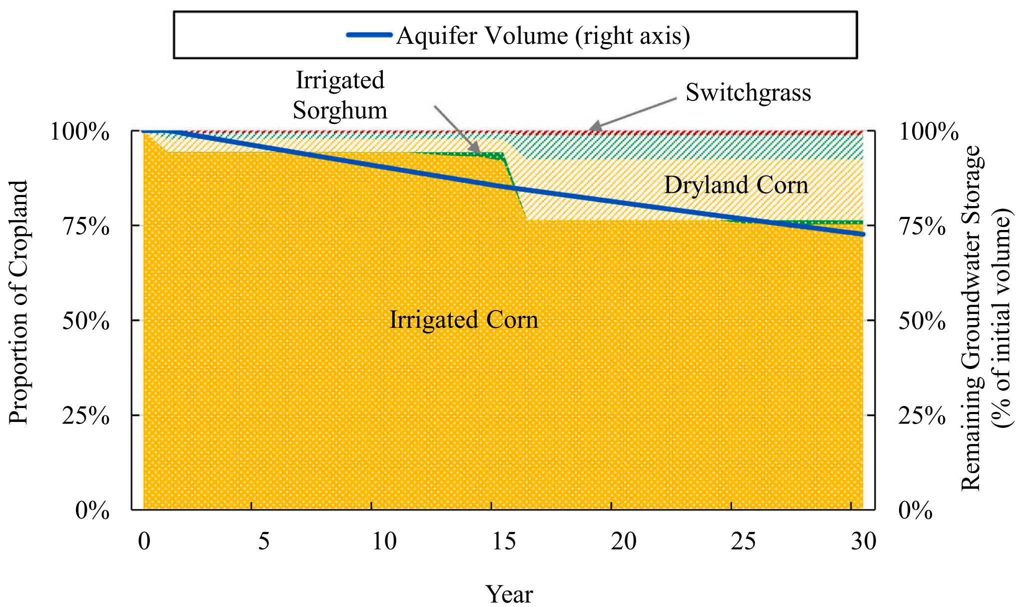

Fig. 6. Change in crop composition and aquifer volume over a 30-year simulation period across the U.S. High Plains Aquifer. The stacked area shows the proportion of cropland allocated to irrigated and dryland crops, including sorghum, and switchgrass. The blue line (right axis) represents the remaining aquifer storage as a percentage of its initial volume . *Note: The discrete change in land-use shares around year 16 reflects synchronized pivot replacement timing under the assumed uniform initial pivot age; this is a modeling artifact rather than a hydrologic threshold.*

intermediate and low-capacity wells continues to rise (26%), further displacing high-capacity wells (48.1% of area). Colorado's initial irrigated area (0.19 million hectares) is similarly dominated by high-capacity wells (90.3%) with 8.4% already economical to be in dryland. By the reinvestment point, the shares of acreage supported by high-capacity wells decline to 85.6% and dryland cultivation edges up to 9.5%, with additional larger transitions subsequently occurring in the latter part of the simulation.

The southern HPA states (Texas, Oklahoma, and New Mexico) undergo the greatest changes to irrigated croplands over the simulation period, with Texas experiencing the largest shifts in well capacities. As in most HPA states, the majority of initial irrigated acreage in Texas is supported by high-capacity wells and dryland agriculture is not a feasible alternative. By the pivot reinvestment stage, the share of land supported by high-capacity wells declines from 86.5% to 54.4% and dryland acreage increases from 0% to 43.3%. At the conclusion of the simulation, well capacities continue to decline.

Oklahoma uniquely experiences a predicted shift in optimal crop mix in year 30 without a shift in irrigated production to low-capacity wells or dryland. At the reinvestment stage, some of the irrigated (maize) production initially supported by high-capacity wells transitions to low-capacity wells. Between year 25 and the end of the simulation period, this area reverts back to production under high-capacity wells, for the cultivation of sorghum rather than maize. In other words, irrigated sorghum production supported by high-capacity wells is able to economically displace maize production supported by intermediate-capacity wells. Lastly, New Mexico not only has a comparatively smaller irrigated baseline area (17,464 ha) but it also has the lowest starting share supported by high-capacity wells (11.5%). Nearly three quarters of irrigated acres in New Mexico can feasibly irrigate at intermediate- to low-capacity wells, and the state has the highest initial share of acreage that is dryland-economical (14.3%). By the reinvestment stage (year 16), the irrigated acreage in New Mexico fully transitions to dryland production, a pattern that persists through year 30.

Overall, the simulations reveal a clear latitudinal gradient in irrigation persistence, with the Northern High Plains maintaining predominantly high-capacity wells, the Central High Plains exhibiting moderate decline, and the Southern High Plains undergoing more extensive shifts toward low-capacity wells and dryland agriculture. Fig. 7 synthesizes the end-of-period outcomes of the study area. By year 30, 66% of remaining irrigated area operates under high-capacity wells (31.5 L s^{-1}), while intermediate and low-capacity wells collectively account for less than 10% of irrigated land (Fig. 7a). Dryland production represents 23% of total cropland formerly under irrigated area, with the majority of this area allocated to dryland maize (65%), followed by dryland sorghum (26%) and a small share of switchgrass (5%) (Fig. 7b). The timing of irrigated-to-dryland transitions across counties is reported in Supplement S6.

3.3. Biomass production, specific crop shifts, and economic impacts

Through the simulation period, irrigated maize production in the HPA region decreases by 3.9% by year 15 and by 21.9% by year 30, falling from an estimated 30.8 Mt yr^{-1} (million tons per year) to 24.2 Mt yr^{-1} (with average yields declining from 11.0 Mg ha^{-1} (163.5 bushels ac^{-1}) to 10.8 Mg ha^{-1} (160.2 bushels ac^{-1})) as the economic viability of center-pivot irrigation wanes. The total biomass production and total net returns over the period of 30 years are shown in Fig. 8a and Fig. 8b, respectively, and vary by region.

Within the Northern High Plains, irrigated maize production remains relatively resilient. Nebraska, which accounts for the largest share of irrigated maize at baseline (19.5 Mt yr^{-1}), experiences a 15.7% decline by year 30–16.4 Mt yr^{-1}. The impact on irrigated maize output in South Dakota is smaller: a reduction of 0.5% from baseline to 30,327 yr^{-1} by year 30. In Wyoming the transitions we model result in a 6.7% reduction in maize production from baseline to 178,984 yr^{-1}. Our model also suggests lower irrigated maize production in the central High Plains. Kansas experiences the sharpest fall in output, of 32.4% from 5.2 Mt yr^{-1} to 3.5 Mt yr^{-1} by year 30. In Colorado, irrigated maize output declines 3.8% to 1.84 Mt yr^{-1}. The Southern High Plains undergo the largest decline in irrigated maize production. Texas irrigated maize production is essentially halved over the simulation period, falling from 3.37 Mt yr^{-1} to 1.68 Mt yr^{-1}, while New Mexico's production is phased out, reflecting the unsustainability of irrigated agriculture where the aquifer is shallow and recharge is limited.

3.3.1. Replacing irrigated maize with irrigated sorghum

Optimal crop allocation shows that irrigated sorghum plays a transitional role during the first 15 years of the simulation under declining irrigation well capacities (Table 2). Starting from a small base of 10,166 yr^{-1} (tonnes per year), irrigated sorghum production increases to 374,458 yr^{-1} by year 15, before declining to 166,563 yr^{-1} by year 30.

This transitional expansion is most prominent in the Central and Southern High Plains. Kansas drives much of the early predicted expansion, with irrigated sorghum rising from 10,166 yr^{-1} to 172,846 yr^{-1} by year 15, before declining to 93,590 yr^{-1} by year 30, a net gain of 820%. Texas exhibits a similar pattern, peaking at 201,590 yr^{-1} in year 15 but declining to 26,747 yr^{-1} by year 30. In Oklahoma, irrigated sorghum production is expected to emerge as optimal only in the final period, producing 46,205 yr^{-1} by year 30, despite no prior production.

3.3.2. Replacement by non-irrigated maize, non-irrigated sorghum, and switchgrass

The projected transitions to dryland cropping systems are summarized in Table 3. Non-irrigated maize is projected to increase in the region by 283.8%, from 835,532 yr^{-1} to 3.2 Mt yr^{-1}, while non-irrigated sorghum grows by 288.7%, from 196,861 yr^{-1} to 765,176 yr^{-1}. These shifts represent a reconfiguration of agricultural systems toward dryland practices, driven by both physical constraints and economic adaptation.

The dryland expansion of maize and sorghum is most pronounced in the Central and Southern High Plains, where irrigation well capacity declines most rapidly. However, Nebraska leads this transition in tonnage to over 2.59 Mt yr^{-1} by year 30—a 210.9% increase. Kansas mirrors this shift for dryland sorghum, increasing more than fourfold, from 137,195 yr^{-1} to 559,233 yr^{-1}. Texas exhibits the most dramatic relative increase in dryland maize, growing from a negligible amount to over 609,000 yr^{-1} by year 30.

Across all states, switchgrass production is anticipated to increase by 35.4%, from 296,260 yr^{-1} to 401,120 yr^{-1} over the 30-year period

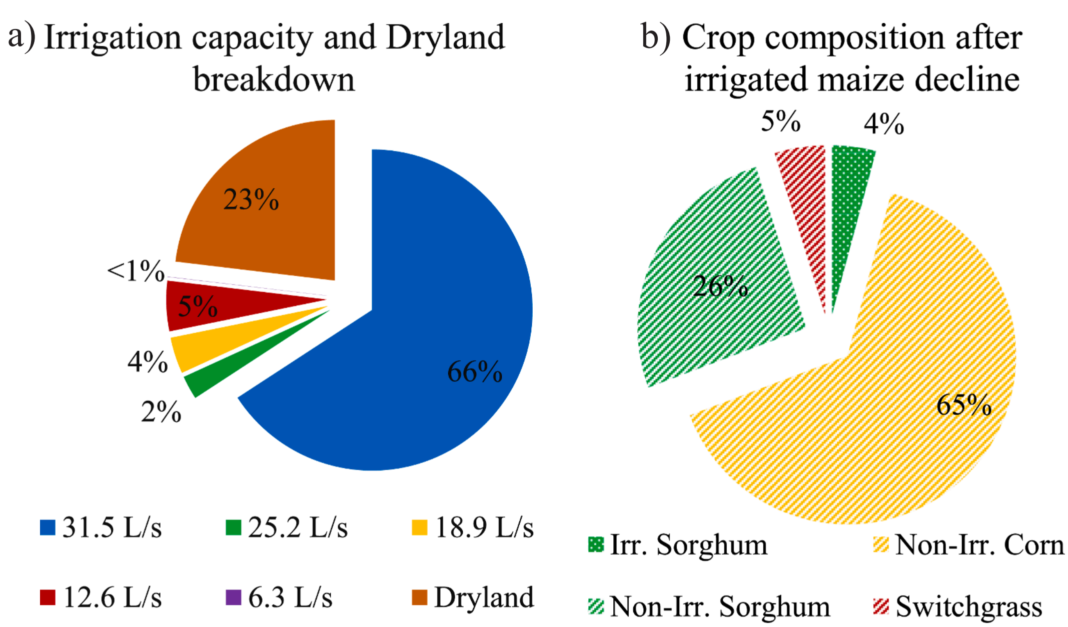

Fig. 7. Change in land use and irrigation use across the U.S. High Plains following irrigated maize area decline. a) Distribution of cropland area by well capacity class (L s^{-1} or L/s) and total dryland extent after 30 years, and b) Share of crops that replace irrigated maize: irrigated sorghum, non-irrigated maize, non-irrigated sorghum, and switchgrass.

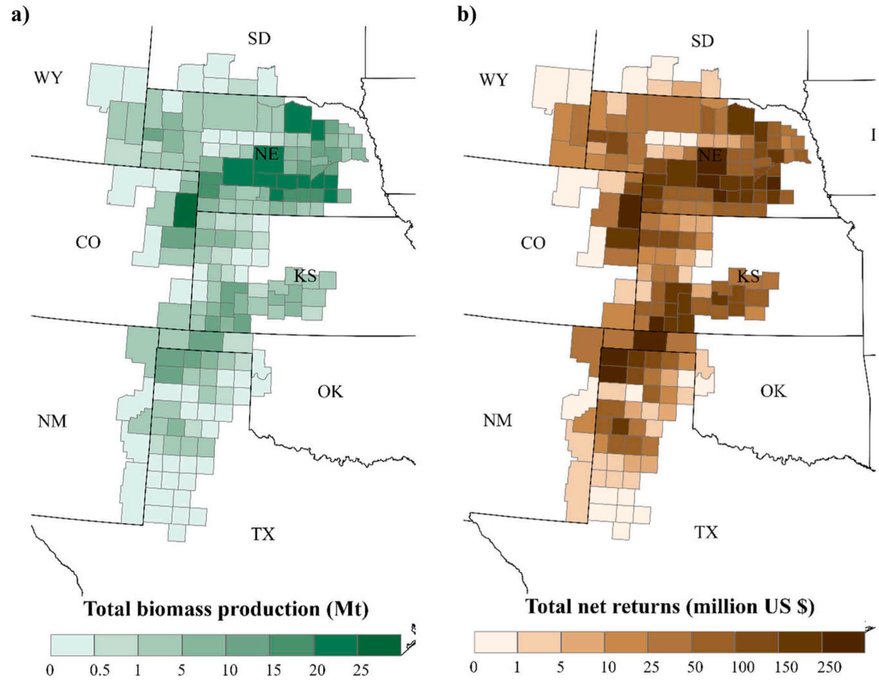

Fig. 8. Distribution of total economic benefits from bioenergy crop production across the U.S. High Plains Aquifer over the 30-year simulation period. a) Cumulative biomass output from all modeled feedstocks, b) Aggregated net present value (NPV) reflecting the spatial variability in profitability driven by groundwater availability and crop productivity.

Table 2
State-level changes in irrigated crop area and production between Year 1 and Year 30 across the U.S. High Plains Aquifer (HPA). Area is reported in hectares (ha) and production in metric tons per year (t yr^{-1}). Regional totals correspond to Northern High Plains (NHP), Central High Plains (CHP), and Southern High Plains (SHP) subregions.

		Area (ha)			Production (t yr^{-1})		
Region / State	**Crop**	**Year 1**	**Year 30**	**Δ Area**	**Year 1**	**Year 30**	**Δ Production**
Northern High Plains							
NE	Maize	1,769,203	1,495,015	−274,188	19,458,574	16,412,886	−3,045,688
SD	Maize	3,306	3,302	−4	30,327	30,162	−165
	Sorghum	0	4	4		20	20
WY	Maize	22,073	22,073	0	178,984	166,962	−12,022
NHP total		1,794,582	1,520,395	−274,187	19,667,885	16,610,030	−3,057,855
Central High Plains							
CO	Maize	172,209	170,234	−1975	1,915,618	1,843,537	−72,081
KS	Maize	465,058	352,097	−112,961	5,201,062	3515,420	−1,685,642
	Sorghum	1,968	16,086	14,118	10,166	93,590	83,424
CHP total		639,235	538,417	−100,818	7,126,846	5,452,547	−1,674,299
Southern High Plains							
TX	Maize	305,121	167,017	−138,104	3,370,325	1,680,645	−1,689,680
	Sorghum	0	5,354	5,354	0	26,747	26,747
NM	Maize	14,965	0	−14,965	133,610	0	−133,160
OK	Maize	50,127	40,948	−9179	523,763	429,586	−94,177
	Sorghum	0	9,179	9,179	0	46,205	46,205
SHP total		370,213	222,498	−147,715	4,027,698	2,183,183	−1,844,065
HPA total		2,804,030	2281,309	−522,721	30,822,429	24,245,760	−6,576,219

under business-as-usual. Although the magnitudes of growth are modest compared to maize, the spatial patterns reveal particularly strong potential in selected areas where neither maize nor sorghum is viable or profitable, such as Colorado and New Mexico. In New Mexico, switchgrass could expand more than six-fold from 16,485 yr^{-1} to 120,367 yr^{-1}, replacing irrigated maize systems that are phased out by year 30. Colorado maintains stable switchgrass production, increasing by 12.9% in year 15 and retaining this level with annual production in year 30 of 113,792 yr^{-1}. County-level crop transitions between the beginning and end of the simulation period are summarized in Supplement S8, and county-level bioenergy biomass production and associated net present value are reported in Supplement S9.

3.4. *Opportunities for bioenergy feedstocks*

The economically viable potential for producing dryland sorghum and switchgrass depends upon the foregone profits associated with their production relative to the current production of irrigated maize (Fig. 9a). Within the Northern High Plains region, opportunity costs for dryland sorghum are lowest (less than $247 ha^{-1} yr^{-1} or $100 ac^{-1} yr^{-1}), indicating a lower but still substantial hurdle for adoption. In these areas, the marginal cost of abandoning irrigation is generally smaller, and in some cases, dryland sorghum may already be competitive with irrigated maize.

In contrast, the Southern High Plains and parts of the Central High

Table 3
State-level changes in non-irrigated crop area and biomass production between Year 1 and Year 30 across the U.S. High Plains Aquifer (HPA). Area is reported in hectares (ha) and production in metric tons per year (t yr^{-1}). Regional totals correspond to Northern High Plains (NHP), Central High Plains (CHP), and Southern High Plains (SHP) subregions.

		Area (ha)			Production (t yr^{-1})		
Region / State	**Crop**	**Year 1**	**Year 30**	**Δ Area**	**Year 1**	**Year 30**	**Δ Production**
Northern High Plains							
NE	Maize	101,602	343,367	241,765	835,491	2,597,188	1,761,697
	Sorghum	12,678	45,101	32,423	59,203	205,481	146,278
WY	Sorghum	123	123	0	463	463	0
NHP total		114,403	388,591	274,188	895,157	2,803,132	1,907,975
Central High Plains							
CO	Switchgrass	15,827	17,802	1,975	100,792	113,792	13,000
KS	Sorghum	30,185	129,028	98,843	137,195	559,233	422,038
CHP total		46,012	146,830	100,818	237,987	673,025	435,038
Southern High Plains							
TX	Maize	9	132,760	132,751	42	609,341	609,299
NM	Switchgrass	2500	17,464	14,964	16,485	120,367	103,882
SHP total		2509	150,224	147,715	16,527	729,708	713,181
HPA total		162,924	685,645	522,721	1,149,671	4,205,865	3,056,194

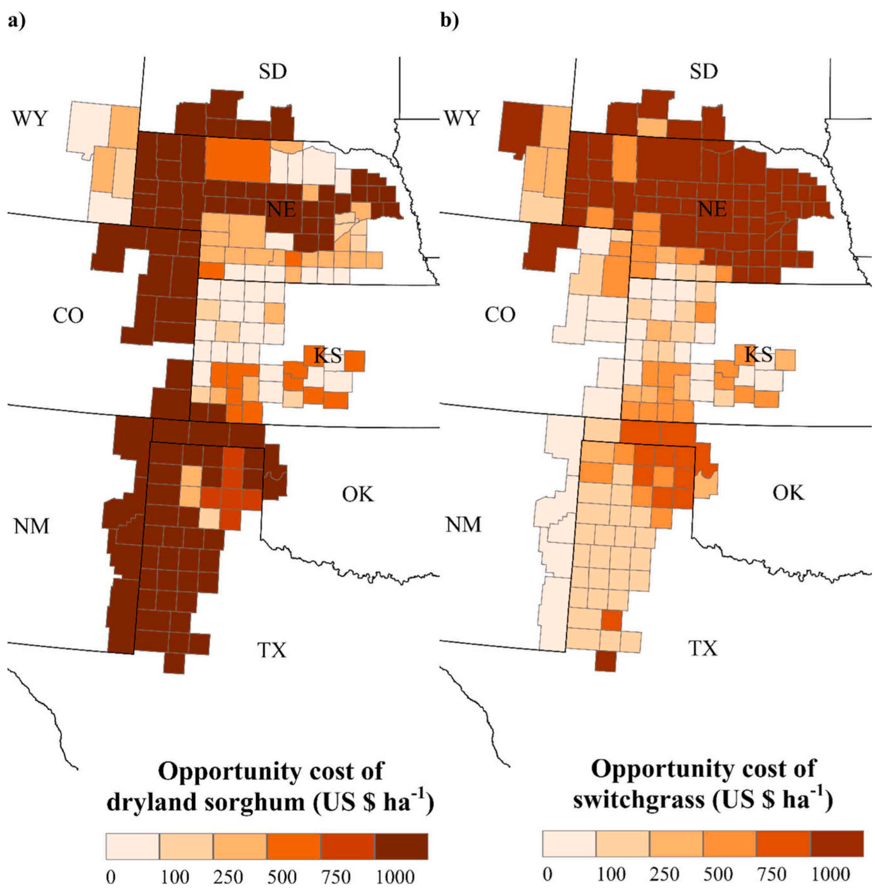

Fig. 9. Spatial variation in opportunity costs for non-irrigated bioenergy feedstocks across the U.S. High Plains Aquifer region. The foregone profit relative to baseline irrigated maize, representing the minimum incentive required for adoption of (a) dryland sorghum b) perennial switchgrass.

Plains exhibit substantially higher opportunity costs ranging from $865 ha^{-1} yr^{-1} ($350 ac^{-1} yr^{-1}) or more, particularly across the Texas High Plains, western Kansas, eastern New Mexico, and much of Oklahoma. Many counties in the Texas High Plains (e.g., Carson, Donley, Gray, Lipscomb, and Wheeler Counties) exceed $741-$988 ha^{-1} yr^{-1} ($300-$400 ac^{-1} yr^{-1}) in estimated opportunity cost, signaling that dryland sorghum adoption would be uncompetitive under current conditions without substantial policy incentives or significant shifts in input/output prices.

The Central High Plains represents a transitional zone, with mixed opportunity costs ($247–741 ha^{-1} yr^{-1}), reflecting moderate yield potential and variable dependence on irrigation. For several counties such as Scott County and Graham County in Kansas, we calculate opportunity costs ranging from $494 ha^{-1} yr^{-1} to $618 ha^{-1} yr^{-1}, suggesting economic viability may be within reach with modest changes in policy, favorable movement in market prices, and technological change.

For switchgrass, the spatial pattern is flipped. Producers in the Northern High Plains face the highest opportunity costs of adopting switchgrass (more than $988 ha^{-1} yr^{-1}) particularly across Nebraska and southern South Dakota. In these counties, the baseline profitability of existing irrigated systems remains high, and switchgrass yields under dryland conditions are relatively low. In portions of the Central High Plains, switchgrass adoption becomes more economically feasible, with opportunity costs below \$100 ha^{-1} yr^{-1} (Fig. 9b).

Counties in the Southern High Plains, particularly in eastern New Mexico, Oklahoma, and the southern Texas High Plains, also have lower opportunity costs (median of \$247 ha^{-1} yr^{-1}). This reflects both lower initial irrigation profitability and more favorable yield performance of perennial systems under groundwater scarcity. Then, in several southern HPA counties (e.g., Briscoe and Parmer in Texas, and Cimarron in Oklahoma) switchgrass emerges as a more cost-effective alternative to irrigated maize than dryland sorghum. County-level opportunity costs and competitiveness indicators for alternative crops are reported in Supplement S10.

4. Discussion

This study integrates hydrologic modeling and economic optimization to evaluate potential cropping transitions under increasing groundwater constraints. By jointly examining water resource availability, crop productivity, and economic viability, we examine agricultural systems that balance profitability and conservation. Our analysis highlights how the complex interplay between aquifer depletion and irrigation use reshapes cropping system dynamics and creates differentiated opportunities for dryland and bioenergy feedstocks.

The spatiotemporal transitions we observe emerge from the interaction of hydrogeological decline, pumping costs, and capital requirements for irrigation infrastructure as represented in the MILP framework. As aquifer transmissivity declines and total pumping head increases, water availability increasingly limits irrigation of water-intensive crops such as maize (Steward et al., 2013, 2009; Steward and Allen, 2016). When the expected net returns fall short of covering the pivot investment cost, irrigation production exits discretely in favor of dryland production. This dynamic of localized depletion is most prominent in the Southern and Central High Plains, where aquifer declines and economic factors converge to accelerate the transition.

Our 30-year simulation indicates that 0.68 million hectares (23%) of current irrigated maize footprint across the High Plains may relinquish center-pivot irrigation, chiefly in the Texas Panhandle and western Kansas, where well capacities fall below the 18.9 L s^{-1} (300 GPM) threshold typically needed for economic reinvestment in those locations. By year 30, Nebraska retains approximately 78% of its initial groundwater volume, whereas Texas retains only 41% – underscoring a strong north-south gradient in aquifer depletion and hydro-economic resilience. The model therefore reinforces the understanding of groundwater depletion not as a uniform decline but as a wave of localized impacts, with vulnerability peaking where transmissivity is low and energy costs increase (Scanlon et al., 2012; Korus and Hensen, 2020).

Our mixed-integer framework embeds a binary *go/no-go* variable of pivot replacement at year 15. More staggered pivot-age and replacement scenarios would show more varied transition timelines but reflect the same general dynamic—once marginal revenues drop below the \$75,000 capital constraint, regions cascade into dryland pathways irrespective of residual saturated thickness. Aggregated discounted profits remain sizeable across our study (US \$12.3 billion over three decades), but 70% accrue in groundwater-rich Nebraska and northern Colorado, revealing how varied sensitivity to groundwater declines and fixed-cost lumpiness of irrigation infrastructure costs amplify geographic inequality in farm income. Policies that reduce the fixed cost of irrigation equipment—such as cost-share programs or low-interest financing—could, in principle, extend the effective life of irrigation systems and delay major reinvestment decisions. Although such policies are not modeled here, the fixed cost structure of the MILP indicates that changes in capital costs would alter the threshold at which irrigation remains economically viable beyond the 15-year replacement cycles (Foster et al., 2017; Pfeiffer and Lin, 2012).

4.1. Persistent decline in irrigated maize

We project that the transition from irrigated maize to dryland production systems will continue as a primary adaptive response to declining aquifer conditions across the High Plains. Region-wide, the share of irrigated area supported by the highest capacity wells falls from 89.0% (year 1) to 75.3% (year 16) and 65.8% (year 30), while currently irrigated areas that can be profitable under dryland cultivation increase from 5.5% (year 1) to 23.1% (year 30). The non-uniform responses in space (e.g., Nebraska sustaining irrigation far longer than Texas or western Kansas) are consistent with documented north-south contrasts in recharge availability and localized depletion in the HPA (Deines et al., 2020; Haacker et al., 2016; McGuire and Strauch, 2024; Mrad et al., 2020). These transitions reflect strategic adjustments not only to physical limitations but also to diminishing economic returns on irrigation infrastructure investments (Pfeiffer and Lin, 2012).

While groundwater depletion drives these patterns, they are also shaped by the relative yield potential of crops under non-irrigated conditions (Irmak, 2015) and the financial viability of reinvesting in pivot systems. States with greater hydrogeological resilience such as Nebraska are able to sustain irrigated maize over multiple investment cycles, whereas areas in Texas and Kansas exhibit earlier and more widespread shifts to dryland crops including maize, sorghum, and switchgrass. Identifying where and when such transitions occur provides a useful benchmark for anticipating the geographic distribution of future irrigation phaseouts and evaluating regionally appropriate crop and water management strategies.

4.2. Irrigated sorghum as an intermediate substitute

The results demonstrate the adaptive but temporary utility of irrigated sorghum under moderate groundwater stress, where partial pivot capacity remains but high-water-demand crops such as maize are no longer viable. The eventual decline of irrigated sorghum by year 30 indicates that even water-efficient irrigated crops are unsustainable in regions where aquifer depletion becomes severe or reinvestment becomes uneconomic.

The temporary expansion of irrigated sorghum—marked by rapid expansion during the first investment period followed by retreat—illustrates its role as an intermediate substitute under groundwater constraints. Irrigated sorghum remains competitive at intermediate well capacities (18.9–25.2 L s^{-1}), where the energy costs associated with groundwater extraction reduce maize profitability. As well capacities decline further, however, irrigated sorghum no longer meets the profitability threshold required for pivot reinvestment and is replaced by dryland systems. This substitution pathway underscores the transitional role of sorghum and aligns with hydro-economic analyses of crop choice and irrigation behavior under declining aquifer dynamic head conditions (Young et al., 2021).

4.3. Rapid growth of non-irrigated systems and the role of switchgrass

The expansion of rainfed production is driven by (i) negative present value for new pivots at the replacement node once the pumping lift requirements and available water are accounted for; (ii) the low switching cost for transitioning to dryland maize, and (iii) soil-climate conditions in subregions (e.g., Nebraska and Central Kansas) where precipitation and soil storage mitigate yield penalties. Empirical evidence from the High Plains indicates that maize becomes less competitive under irrigation deficits, whereas dryland production can remain a viable alternative (Payero et al., 2006). Consistent with these observations, our optimization model transitions cropland from irrigated to dryland production at the reinvestment decision point when irrigation is no longer economically optimal. The resulting land-use configuration then remains relatively stable over the remainder of the planning horizon.

Within this transition, dryland sorghum plays a central role in counties where rainfall reliability, soils with adequate plant-available water, and temperature regimes collectively support stable grain production under deficit conditions (Colaizzi et al., 2004; Klocke et al., 2009). Sorghum's lower seasonal evapotranspiration, deeper rooting, and tolerance to intra-seasonal water stress reduce yield volatility relative to dryland maize under similar conditions (Staggenborg et al., 2008). Economically, this translates into water-efficient productivity and lower risk when seasonal precipitation is uncertain (Dhuyvetter et al., 1996; Pfeiffer and Lin, 2014). In our results, Kansas is the leading example, where dryland sorghum expands by 308% by year 30, displacing irrigated maize first at the reinvestment node and then persisting as a low-capital and water-resilient system.

Perennial bioenergy crops expand selectively where opportunity costs are low and irrigation is already retired. Switchgrass cultivation increases 35% region-wide, with particularly large proportional gains where irrigation exits early. The adoption of switchgrass represents an emerging opportunity for perennial bioenergy systems within broader agroecological transitions. These systems may offer co-benefits in terms of soil conservation, improved carbon sequestration, and enhanced land resilience, while also diversifying farm income in regions facing long-term groundwater depletion, consistent with the sustainability benefits reported for perennial bioenergy systems (Hamilton et al., 2015; Robertson et al., 2017; Tiemann and Grandy, 2015). For switchgrass to be adopted, its net returns must exceed those of the competing dryland alternatives—primarily dryland sorghum and dryland maize.

Opportunity cost mapping shows that in the southern High Plains especially eastern New Mexico and the southern Texas Panhandle switchgrass out-competes dryland sorghum when opportunity costs fall below \$247 ha^{-1} yr^{-1}. Central Nebraska, by contrast, presents the converse pattern, favoring sorghum due to dryland yields. Across the entire High Plains region, 31% of the land exiting irrigation transitions to the potential bioenergy crops of sorghum and switchgrass, offering a consistent biomass supply with no new water withdrawals. The spatial bifurcation of their adoption locations identifies areas where future scenario analysis could evaluate whether carbon pricing, biomass incentives, or ecosystem-service payments would affect perennial adoption, particularly where opportunity costs are already relatively low (Clifton-Brown et al., 2023).

Future scenario analysis could also examine how conservation cost-share programs or bioenergy procurement contracts might affect adoption economics in these areas. Notably, central Colorado and portions of eastern Wyoming show moderate opportunity costs (\$247–618 ha^{-1} yr^{-1}), making switchgrass marginally viable depending on local cost structure and market access. This spatial pattern likely reflects the economic conditions represented in the model, where increasing pumping costs and declining irrigation returns favor transitions to switchgrass in areas where perennial production remains economically competitive. Switchgrass's deep root systems, drought tolerance, and low input requirements further enhance its suitability under these conditions. Comparing the maps of sorghum and switchgrass opportunity costs reveals a striking spatial divergence in relative feasibility. Central Nebraska and northeastern Colorado show low opportunity costs for dryland sorghum but high costs for switchgrass, suggesting a clear preference for annual dryland cropping systems. In contrast, southern Texas Panhandle and eastern New Mexico show the inverse, favoring switchgrass over sorghum due to low yields and better perennial biomass performance. This spatial contrast identifies an intermediate transition zone across central Kansas and eastern Colorado, where opportunity costs for both crops are moderate (\$247–618 ha^{-1} yr^{-1}). In these mixed-feasibility zones, crop producers may evaluate crop choice based on rotational preferences, risk aversion and available subsidies. These regions are likely to be most responsive to incremental changes in market signals. The results also identify "resistant zones" where high opportunity cost for both crops (more than \$988 ha^{-1} yr^{-1}) prevail. These include the core irrigated regions of central Nebraska and some areas of the Texas High Plains where neither dryland sorghum nor switchgrass is currently economically viable. These areas face the highest risk of abrupt productivity loss if irrigation becomes unsustainable.

4.4. Synthesis

Under the modeled land-use allocation pathway, dynamic shifts from the highest capacity wells (31.5 L s^{-1}) toward lowest-capacity wells (6.3 L s^{-1}) and dryland production are associated with conserving more than one-third of initial groundwater in the HPA that would otherwise be exhausted under static management. Yet rising pumping lift costs still reduce net returns in the southern High Plains, showing that demand-side efficiency must be paired with lower energy costs to stabilize the farm margins (Steward et al., 2009). Our model's coupling of hydraulic strata with depth-specific pumping coefficients provides a foundation for future energy-water-trade-off analyses under climate and policy scenarios.

Our work illustrates the value of analyzing alternative agricultural land use pathways to help prolong the life of the HPA. The modeled transitions to dryland and less water-intensive cropping systems identify where biomass feedstock production may become economically competitive as irrigation constraints intensify, while also showing where irrigated maize remains comparatively resilient.

Our findings should be interpreted as model-implied transition pathways under the stated assumptions rather than as prescriptions for producer or policy action. Because policy instruments, groundwater regulation, biomass contracts, and stakeholder behavior are not modeled directly, the results are best viewed as a spatial benchmark for future analysis. Nevertheless, the heterogeneity in hydrogeologic conditions and economic returns indicate that uniform policy instruments, whether implemented through aquifer-wide management districts or broader regional authorities, could distribute costs and benefits unevenly across the HPA. Future policy evaluations should therefore examine how alternative management approaches perform under locally varying groundwater conditions, crop opportunities, and reinvestment thresholds.

The transferability of local groundwater-management approaches also warrants careful evaluation. Orduña Alegría et al. (2024), for example, report that the groundwater-conservation outcomes achieved through Kansas's SD−6 LEMA were not readily replicated in nearby jurisdictions. More broadly, our findings reinforce the view that sustainable irrigation in HPA is a complex governance challenge rather than a problem with a single techno-economic or regulatory panacea (Ostrom et al., 2007; Meinzen-Dick, 2007). In this context, the spatial patterns identified here provide a foundation for future evaluation of multi-scale, trajectory-based governance approaches such as those outlined by Schipanski et al. (2023).

4.5. Limitations and uncertainty

In our optimization framework, we treat each county as a single-cell aquifer with homogeneous hydraulic properties and no lateral fluxes. This assumption maintains tractability across 180 counties, but it masks fine-scale heterogeneity in saturated thickness, transmissivity, and irrigation drawdown that influence well performance at the field scale. Consequently, the maps created may over- or under-state trajectories where local transmissivity differs from county means. Incorporating cell-to-cell leakage or fully coupled groundwater flow models (e.g., MODFLOW) could potentially address this concern in future work (Langevin et al., 2026).

In our current work, aquifer attributes derived from raster products (GLHYMPS permeability, USGS saturated thickness, and LANID irrigation masks) had a native resolution of 500 m and were aggregated to county means. Errors due to mixed pixels, noise, and extrapolation of well data could propagate into effective well-capacity classes used to estimate yield response functions. A ± 10% error in saturated thickness also introduces an associated error in the drawdown cost coefficient, and this uncertainty is not reflected in the deterministic MILP.

All simulations hold annual recharge, growing season precipitation, and evapotranspiration demand at their recent climatological means. They therefore omit two sources of uncertainty that are likely to grow over the 30-year horizon: (i) intensifying summer aridity across the southern High Plains, and (ii) the coincident tendency for extreme rainfall events to increase recharge non-linearly. Either process could accelerate or dampen the decline in effective irrigation capacities shown in Fig. 4. In regions such as the Northern High Plains, where irrigation has expanded historically, allowing irrigation expansion in the model could alter projected groundwater outcomes. Incorporating endogenous irrigation expansion would be an important extension for future work.

Relative yield curves for maize and sorghum were fitted to four experimental sites (western CO, western KS, SW NE, and TX High Plains) and then applied uniformly across the entire HPA region. While piecewise linearization captures first-order biophysical responses, it ignores environmental interactions and soil textural effects. In regions with heavier soils or late maturing hybrids, the model may underpredict yields at low pumping rates; in early maturity regions it may overpredict.

Peripheral counties with less than 100 km^2 overlying the aquifer were excluded to ensure analytical relevance. Although these counties represent less than 4% of the total irrigated maize, they tend to exhibit lower irrigation intensity compared to the core irrigated zones. Their exclusion may introduce modest bias in the average depletion rates for the study area. The MILP also yields a single "most effective" solution for each county under the assumed parameters, and we did not propagate parameters of uncertainty through weather or price shocks. Future work should adopt stochastic dynamic programming or robust optimization to generate decision spaces that account for such parameter and process uncertainties.

Our use of a common budget structure from Kansas State University extension ensures consistent production costs for all counties featured in our model. Although this avoids the introduction of additional uncertainty from inconsistent or incomplete data, the costs remain most closely representative of Kansas and actual costs may deviate from these estimates in other HPA states.

The analysis assumes (i) a real discount rate of 7%, (ii) 2018–2023 average commodity prices and input costs were held constant in real terms, and (iii) a fixed $75,000 capital cost for a new center-pivot that is replaced exactly in year 16. This approach slightly inflates the initial investment cost and does not precisely reflect current infrastructure realities, but the influence of this assumption diminishes significantly over multiple pivot replacement cycles. Sensitivity tests by adjusting discount rate and future prices may not overturn the qualitative ranking of the regions, but they could shift the timing of the pivot system investment. Furthermore, pumping energy requirements were calculated with depth-specific (kWh m^{-3}) coefficients, but natural gas prices were held at the 2023 average. We neither factor in costs of CO_2 emissions (e.g., a carbon tax) from pumping, nor consider potential soil carbon benefits and credits from switching to perennial cover (switchgrass). Internalizing these externalities would favor lower-energy use systems and perennial feedstocks, but the magnitude is policy-contingent and therefore excluded.

We assume no new groundwater use regulations, no changes to the Renewable Fuel Standard or other energy policies like a Clean Fuel Program, and no dedicated biomass supply contracts. A stricter pumping limitation, a carbon fuel standard, or perennial-crop incentives could accelerate the transitions forecasted; conversely, subsidized irrigation energy programs could delay them.

Finally, we caution against extrapolating the absolute magnitudes of land-use change beyond the 30-year horizon. For example, the pivot-replacement schedule, aquifer drawdown, and technological advances (e.g., subsurface drip or deficit irrigation algorithms) will interact in ways that cannot be forecasted linearly. Our estimates are intentionally conservative, and the overall limitations and uncertainties of the current model underscore that they are best viewed as directional rather than predictive. They serve to bound the problem, and also highlight where improved data (e.g., high-resolution recharge rates, county-level pivot age) could most reduce uncertainty, improve decision-making, and provide a transparent platform for scenario testing under alternative weather, market, or policy futures.

5. Conclusions

This study develops a spatial hydro-economic optimization framework to examine the long-term optimal allocation of cropping systems in irrigated agriculture across the U.S. HPA under groundwater constraints. By integrating county-level hydrogeologic conditions, depth-dependent pumping costs, and net returns to crop production over a 30-year horizon, we evaluate how irrigated maize systems adjust through shifts in well capacity, crop substitution, and transitions to dryland production. We find pronounced spatial heterogeneity in resilience of irrigated agriculture: irrigation remains comparatively robust in portions of the Northern High Plains, whereas counties in the Central and Southern High Plains experience earlier contraction of high-capacity wells and greater shifts toward dryland systems. Approximately 0.69 million hectares transition from irrigated to dryland production over the simulation period, with irrigated sorghum functioning primarily as an intermediate land use under moderate capacity constraints and perennial bioenergy crops expanding selectively where opportunity costs are low.

These findings are important for three reasons. First, they demonstrate that groundwater depletion induces gradual but regionally differentiated adjustments rather than uniform changes. Second, they quantify the scale and timing of irrigation contraction under economically rational adaptation, providing a benchmark against which observed behavioral responses can be evaluated. Finally, they identify locations where policy interventions such as managed aquifer depletion, irrigation efficiency programs, or support for lower water use cropping systems may (or may not) effectively balance farm profitability with long-term groundwater sustainability. Together, the results underscore that pathways of adaptation to declining groundwater are spatially contingent, and that economically optimal transitions can inform water management strategies in over-extracted aquifer systems globally.

CRediT authorship contribution statement

Tyler J. Lark: Writing – review & editing, Supervision, Software, Project administration, Funding acquisition, Conceptualization. **Nazli Uludere Aragon:** Writing – review & editing, Visualization, Supervision, Resources, Data curation. **Karthik Ramaswamy:** Writing – original draft, Visualization, Validation, Resources, Methodology, Investigation, Formal analysis, Data curation, Conceptualization.

Declaration of Competing Interest

The authors declare that they have no known competing financial interests or personal relationships that could appear to influence the work reported in this paper.

Acknowledgements

This material is based upon work supported by the Great Lakes Bioenergy Research Center, U.S. Department of Energy, Office of Science, Office of Biological and Environmental Research (award number DE-SC0018409).

Appendix A. Supporting information

Supplementary data associated with this article can be found in the online version at doi:10.1016/j.agwat.2026.110675.

Data availability

Data will be made available on request.

References

Abraha, M., Gelfand, I., Hamilton, S.K., Shao, C., Su, Y.-J., Robertson, G.P., Chen, J., 2016. Ecosystem water-use efficiency of annual corn and perennial grasslands: contributions from land-use history and species composition. Ecosystems 19, 1001–1012. https://doi.org/10.1007/s10021-016-9981-2.

Abramowitz, M., Stegun, I.A., 1964. Handbook of mathematical functions with formulas, graphs, and mathematical tables. Applied Mathematics Series. Dover Publications, New York, USA.

Alley, W.M., Reilly, T., Franke, O., 1999. Sustainability of ground-water resources (Report No. 1186). Circular. https://doi.org/10.3133/cir1186.

Araya, A., Gowda, P.H., Golden, B., Foster, A.J., Aguilar, J., Currie, R., Ciampitti, I.A., Prasad, P.V.V., 2019. Economic value and water productivity of major irrigated crops in the Ogallala aquifer region. Agric. Water Manag. 214, 55–63. https://doi.org/10.1016/j.agwat.2018.11.015.

Blanco-Canqui, H., 2016. Growing dedicated energy crops on marginal lands and ecosystem services. Soil. Sci. Soc. Am. J. 80, 845–858. https://doi.org/10.2136/sssaj2016.03.0080.

Brandes, E., Plastina, A., Heaton, E.A., 2018. Where can switchgrass production be more profitable than corn and soybean? An integrated subfield assessment in Iowa, USA. GCB Bioenergy 10, 473–488. https://doi.org/10.1111/gcbb.12516.

Bredehoeft, J.D., Young, R.A., 1970. The temporal allocation of ground water—a simulation approach. Water Resour. Res. 6, 3–21. https://doi.org/10.1029/WR006i001p00003.

Brozović, N., Sunding, D.L., Zilberman, D., 2010. On the spatial nature of the groundwater pumping externality. Spat. Nat. Resour. Environ. Econ. 32, 154–164. https://doi.org/10.1016/j.reseneeco.2009.11.010.

Chowdhury, P., Mahi, N.A., Yeassin, R., Chowdhury, N.-U.-R., Farrok, O., 2025. Biomass to biofuel: Impacts and mitigation of environmental, health, and socioeconomic challenges. Energy Convers. Manag. X 25, 100889. https://doi.org/10.1016/j.ecmx.2025.100889.

Clifton-Brown, J., Hastings, A., von Cossel, M., Murphy-Bokern, D., McCalmont, J., Whitaker, J., Alexopoulou, E., Amaducci, S., Andronic, L., Ashman, C., Awty-Carroll, D., Bhatia, R., Breuer, L., Cosentino, S., Cracroft-Eley, W., Donnison, I., Elbersen, B., Ferrarini, A., Ford, J., Greef, J., Ingram, J., Lewandowski, I., Magenau, E., Mos, M., Petrick, M., Pogrzeba, M., Robson, P., Rowe, R.L., Sandu, A., Schwarz, K.-U., Scordia, D., Scurlock, J., Shepherd, A., Thornton, J., Trindade, L.M., Vetter, S., Wagner, M., Wu, P.-C., Yamada, T., Kiesel, A., 2023. Perennial biomass cropping and use: Shaping the policy ecosystem in European countries. GCB Bioenergy 15, 538–558. https://doi.org/10.1111/gcbb.13038.

Colaizzi, P.D., Schneider, A.D., Evett, S.R., Howell, T.A., 2004. Comparison of SDI, LEPA, and spray irrigation performance for grain sorghum. Trans. ASAE 47, 1477–1492. https://doi.org/10.13031/2013.17628.

Cooper, H.H., Jacob, C., 1946. A generalized graphical method for evaluating formation constants and summarizing well-field history. Eos Trans. Am. Geophys. Union. 27, 526–534. https://doi.org/10.1029/TR027i004p00526.

Cui, X., Kavvada, O., Huntington, T., Scown, C.D., 2018. Strategies for near-term scale-up of cellulosic biofuel production using sorghum and crop residues in the US. Environ. Res. Lett. 13, 124002. https://doi.org/10.1088/1748-9326/aae6e3.

Daly, C., Halbleib, M.D., Hannaway, D.B., Eaton, L.M., 2018. Environmental limitation mapping of potential biomass resources across the conterminous United States. GCB Bioenergy 10, 717–734. https://doi.org/10.1111/gcbb.12496.

Dasgupta, P.S., Heal, G.M., 1979. Economic Theory and Exhaustible Resources. Cambridge University Press.

Deines, J.M., Schipanski, M.E., Golden, B., Zipper, S.C., Nozari, S., Rottler, C., Guerrero, B., Sharda, V., 2020. Transitions from irrigated to dryland agriculture in the Ogallala Aquifer: land use suitability and regional economic impacts. Agric. Water Manag. 233, 106061. https://doi.org/10.1016/j.agwat.2020.106061.

Dhuyvetter, K.C., Thompson, C.R., Norwood, C.A., Halvorson, A.D., 1996. Economics of dryland cropping systems in the great plains: a review. J. Prod. Agric. 9, 216–222. https://doi.org/10.2134/jpa1996.0216.

Dieter, C., Maupin, M., Caldwell, R., Harris, M., Ivahnenko, T., Lovelace, J., Barber, N., Linsey, K., 2018. Estimated use of water in the United States in 2015 (Report No. 1441). Circ. Rest. VA. https://doi.org/10.3133/cir1441.

Fingerman, K.R., Torn, M.S., O'Hare, M.H., Kammen, D.M., 2010. Accounting for the water impacts of ethanol production. Environ. Res. Lett. 5, 014020. https://doi.org/10.1088/1748-9326/5/1/014020.

Foster, T., Brozović, N., Speir, C., 2017. The buffer value of groundwater when well yield is limited. J. Hydrol. 547. https://doi.org/10.1016/j.jhydrol.2017.02.034.

Frisvold, G.B., Deva, S., 2012. Farm size, irrigation practices, and conservation program participation in the US Southwest. Irrig. Drain. 61, 569–582. https://doi.org/10.1002/ird.1676.

Gisser, M., Mercado, A., 1972. Integration of the agricultural demand function for water and the hydrologic model of the Pecos Basin. Water Resour. Res. 8, 1373–1384. https://doi.org/10.1029/WR008i006p01373.

Gleeson, T., Moosdorf, N., Hartmann, J., van Beek, L.P.H., 2014. A glimpse beneath earth's surface: GLobal HYdrogeology MaPS (GLHYMPS) of permeability and porosity. Geophys. Res. Lett. 41, 3891–3898. https://doi.org/10.1002/2014GL059856.

Griffith, A., Haque, M., Epplin, F.M., 2014. Cost to produce and deliver cellulosic feedstock to a biorefinery: switchgrass and forage sorghum. Appl. Energy 127, 44–54. https://doi.org/10.1016/j.apenergy.2014.03.068.

Haacker, E.M.K., Kendall, A.D., Hyndman, D.W., 2016. Water level declines in the high plains aquifer: predevelopment to resource senescence. Groundwater 54. https://doi.org/10.1111/gwat.12350.

Hamilton, S.K., Hussain, M.Z., Bhardwaj, A.K., Basso, B., Robertson, G.P., 2015. Comparative water use by maize, perennial crops, restored prairie, and poplar trees in the US Midwest. Environ. Res. Lett. 10, 064015. https://doi.org/10.1088/1748-9326/10/6/064015.

Hecox, G.R., Macfarlane, P.A., Wilson, B.B., 2002. Calculation of yield for high plains wells: relationship between saturated thickness and well yield (Open File No. 2002–25 C), technical support for ogallala aquifer assessment, planning, and management. Kans. Geol. Surv.

Hornbeck, R., Keskin, P., 2014. The historically evolving impact of the Ogallala Aquifer: agricultural adaptation to groundwater and drought. Am. Econ. J. Appl. Econ. 6, 190–219. https://doi.org/10.1257/app.6.1.190.

Hotelling, H., 1931. The economics of exhaustible resources. J. Polit. Econ. 39, 137–175. http://www.jstor.org/stable/1822328.

Irmak, S., 2015. Interannual variation in long-term center pivot–irrigated maize evapotranspiration and various water productivity response indices. I: grain yield, actual and basal evapotranspiration, irrigation-yield production functions, evapotranspiration-yield production functions, and yield response factors. J. Irrig. Drain. Eng. 141, 04014068. https://doi.org/10.1061/(ASCE)IR.1943-4774.0000825.

Kansas State University, 2024. *Farm Budgets*. AgManager.info. Kansas State University Department of Agricultural Economics. https://agmanager.info/farm-budgets (Available at).

Kansas State University Department of Agronomy, 2026. Double Crop Options after Wheat. Agronomy eUpdate, Issue 1105, May 28, 2026. Kansas State University, Manhattan, KS. https://www.agronomy.k-state.edu/eupdates/2026/issue-1105-may-28/double-crop-options-after-wheat.html (Available at).

Klocke, N.L., Currie, R.S., Aiken, R.M., 2009. Soil water evaporation and crop residues. Trans. ASABE 52, 103–110. https://doi.org/10.13031/2013.25951.

Klocke, N.L., Currie, R.S., Tomsicek, D.J., Koehn, J., 2011. Corn yield response to deficit irrigation. Trans. ASABE 54, 931–940. https://doi.org/10.13031/2013.37118.

Klocke, N.L., Currie, R.S., Tomsicek, D.J., Koehn, J.W., 2012. Sorghum yield response to deficit irrigation. Trans. ASABE 55, 947–955. https://doi.org/10.13031/2013.41526.

Korus, J.T., Hensen, H.J., 2020. Depletion percentage and nonlinear transmissivity as design criteria for groundwater-level observation networks. Environ. Earth Sci. 79, 382. https://doi.org/10.1007/s12665-020-09123-y.

Kranz, W., Martin, D.L., Patterson, D., Hudgins, J., van Donk, S., Yonts, C.D., 2010. Updating the Nebraska pumping plant performance criteria. Proceedings of the Central Plains Irrigation Conference. https://digitalcommons.unl.edu/biosysengpres/72/.

Lamm, F.R., O'Brien, D.M., Rogers, D.H., 2015. Economic comparison of subsurface drip and center pivot sprinkler irrigation using spreadsheet software. Appl. Eng. Agric. 31, 929–936. https://doi.org/10.13031/aea.31.11253.

Lamm, F.R., Stone, L.R., O'Brien, D.M., 2007. Crop production and economics in northwest Kansas as related to irrigation capacity. Appl. Eng. Agric. 23, 737–745. https://doi.org/10.13031/2013.24057.

Langevin, C.D., Hughes, J.D., Provost, A.M., Russcher, M.J., Morway, E.D., Reno, M.J., Bonelli, W.P., Niswonger, R.G., Panday, S., Titus, S., Merrick, D., Banta, E.R., 2026. MODFLOW 6 Modular Hydrologic Model version 6.7.0: U.S. Geol. Surv. Softw. Release 6 Febr. 2026. https://doi.org/10.5066/P1IJAXDZ.

McGuire, V.L., 2013. Water-level and storage changes in the High Plains aquifer, predevelopment to 2011 and 2009-11 (Report No. 2012–5291), Scientific Investigations Report. Rest. VA. https://doi.org/10.3133/sir20125291.

McGuire, V.L., 2014. Water-level changes and change in water in storage in the High Plains aquifer, predevelopment to 2013 and 2011-13 (Report No. 2014–5218), Scientific Investigations Report. Rest. VA. https://doi.org/10.3133/sir20145218.

McGuire, V.L., 2017. Data used to map water-level changes in the high plains aquifer, predevelopment (about 1950) to 2015 and 2013–2015. US Geol. Surv. Data Release. https://doi.org/10.5066/F7SB43WM.

McGuire, V., Lund, K., Densmore, B., 2012. Saturated thickness and water in storage in the High Plains aquifer, 2009, and water-level changes and changes in water in storage in the High Plains aquifer, 1980–1995, 1995–2000, 2000–2005, and 2005–2009 (Report No. 2012–5177), Scientific Investigations Report. Rest. VA. https://doi.org/10.3133/sir20125177.

McGuire, V.L., Strauch, K.R., 2022. Water-level and recoverable water in storage changes, High Plains aquifer, predevelopment to 2017 and 2015–17 (Report No. 2022–5080), Scientific Investigations Report. Rest. VA. https://doi.org/10.3133/sir20225080.

McGuire, V.L., Strauch, K.R., 2024. Water-level and recoverable water in storage changes, High Plains Aquifer, predevelopment to 2019 and 2017–2019 (Report No. 2023–5143), Scientific Investigations Report. Rest. VA. https://doi.org/10.3133/sir20235143.

Meinzen-Dick, R., 2007. Beyond panaceas in water institutions. In: Proceedings of the National Academy of Sciences, 104, pp. 15200–15205. https://doi.org/10.1073/pnas.0702296104.

Morris, S., Persons, T., 2019. Irrigated Agriculture: Technologies, Practices, and Implication for Water Scarcity (Technology Assessment No. GAO-20-128SP). United States Government Accountability Office, Washington, DC.

Mrad, A., Katul, G.G., Levia, D.F., Guswa, A.J., Boyer, E.W., Bruen, M., Carlyle-Moses, D. E., Coyte, R., Creed, I.F., van de Giesen, N., Grasso, D., Hannah, D.M., Hudson, J.E., Humphrey, V., Iida, S., Jackson, R.B., Kumagai, T., Llorens, P., Michalzik, B., Nanko, K., Peters, C.A., Selker, J.S., Tetzlaff, D., Zalewski, M., Scanlon, B.R., 2020. Peak grain forecasts for the US high plains amid withering waters. Proc. Natl. Acad. Sci. USA 117, 26145–26150. https://doi.org/10.1073/pnas.2008383117.

New, L., Fipps, G., 2000. Center pivot irrigation. Texas Agricultural Extension Service. Texas A&M University System. Bull. B-6096 20. https://texaslocalproduce.tamu.edu/files/2023/08/B-6096-Center-Pivot-Irrigation.pdf.

O'Brien, D.M., Rogers, D.H., Lamm, F.R., Clark, G.A., 1998. An economic comparison of subsurface drip and center pivot sprinkler irrigation systems. Appl. Eng. Agric. 14, 391–398. https://doi.org/10.13031/2013.19401.

Orduña Alegría, M.E., Zipper, S., Shin, H.C., Deines, J.M., Hendricks, N.P., Allen, J.J., Bohling, G.C., Golden, B., Griggs, B.W., Lauer, S., Lin, C.-Y., Marston, L.T., Sanderson, M.R., Smith, S.M., Whittemore, D.O., Wilson, B.B., Yu, D.J., Yu, Q.C., Butler, J.J., 2024. Unlocking aquifer sustainability through irrigator-driven groundwater conservation. Nat. Sustain. 7, 1574–1583. https://doi.org/10.1038/s41893-024-01437-0.

Ostrom, E., Janssen, M.A., Anderies, J.M., 2007. Going beyond panaceas. In: Proceedings of the National Academy of Sciences, 104, pp. 15176–15178. https://doi.org/10.1073/pnas.0701886104.

Payero, J.O., Melvin, S.R., Irmak, S., Tarkalson, D., 2006. Yield response of corn to deficit irrigation in a semiarid climate. Agric. Water Manag. 84, 101–112. https://doi.org/10.1016/j.agwat.2006.01.009.

Perez-Quesada, G., Hendricks, N.P., Steward, D.R., 2024. The economic cost of groundwater depletion in the high plains aquifer. J. Assoc. Environ. Resour. Econ. 11, 253–285. https://doi.org/10.1086/726156.

Pfeiffer, L., Lin, C.-Y.C., 2012. Groundwater pumping and spatial externalities in agriculture. J. Environ. Econ. Manag. 64, 16–30. https://doi.org/10.1016/j.jeem.2012.03.003.

Pfeiffer, L., Lin, C.-Y.C., 2014. Does efficient irrigation technology lead to reduced groundwater extraction? Empirical evidence. J. Environ. Econ. Manag. 67, 189–208. https://doi.org/10.1016/j.jeem.2013.12.002.

Ramaswamy, K., 2016. Economics of Irrigated Crop Choices Using Center Pivot System in Oklahoma Panhandle (M.S.). ProQuest Diss. Theses. Oklahoma State University, Stillwater, Oklahoma.

Ramaswamy, K., 2024. Economic Strategies to Synergistically Produce Bioenergy and Optimize Aquifer Life in the US High Plains. Sel. Pap. Presente Agric. & Appl. Econ. Assoc. Annu. Meet. New. Orleans LA.

Rao, M.N., Yang, Z., 2010. Groundwater impacts due to conservation reserve program in Texas County, Oklahoma. Appl. Geogr. 30, 317–328. https://doi.org/10.1016/j.apgeog.2009.08.006.

Reynolds, S., Guerrero, B., Golden, B., Amosson, S., Marek, T., Bell, J.M., 2020. Economic feasibility of conversion to mobile drip irrigation in the Central Ogallala region. Irrig. Sci. 38, 569–575. https://doi.org/10.1007/s00271-020-00667-2.

Roberts, M.J., Lubowski, R.N., 2007. Enduring impacts of land retirement policies: evidence from the conservation reserve program. Land. Econ. 83, 516. https://doi.org/10.3368/le.83.4.516.

Robertson, G.P., Hamilton, S.K., Barham, B.L., 2017. Cellulosic biofuel contributions to a sustainable energy future: choices and outcomes. Science 356 (6345), eaal2324. https://doi.org/10.1126/science.aal2324.

Rudnick, D.R., Irmak, S., West, C., Chávez, J.L., Kisekka, I., Marek, T.H., Schneekloth, J. P., Mitchell McCallister, D., Sharma, V., Djaman, K., Aguilar, J., Schipanski, M.E., Rogers, D.H., Schlegel, A., 2019. Deficit irrigation management of maize in the high plains aquifer region: a review. JAWRA J. Am. Water Resour. Assoc. 55, 38–55. https://doi.org/10.1111/1752-1688.12723.

Sampson, G.S., Hendricks, N.P., Taylor, M.R., 2019. Land market valuation of groundwater. Resour. Energy Econ. 58, 101120. https://doi.org/10.1016/j.reseneeco.2019.101120.

Scanlon, B.R., Faunt, C.C., Longuevergne, L., Reedy, R.C., Alley, W.M., McGuire, V.L., McMahon, P.B., 2012. Groundwater depletion and sustainability of irrigation in the US High Plains and Central Valley. Proc. Natl. Acad. Sci. USA 109, 9320–9325. https://doi.org/10.1073/pnas.1200311109.

Schipanski, M.E., Sanderson, M.R., Méndez-Barrientos, L.E., Kremen, A., Gowda, P., Porter, D., Wagner, K., West, C., Rice, C.W., Marsalis, M., Guerrero, B., Haacker, E., Dobrowolski, J., Ray, C., Auvermann, B., 2023. Moving from measurement to governance of shared groundwater resources. Nat. Water 1, 30–36. https://doi.org/10.1038/s44221-022-00008-x.

Schloss, J.A., Buddemeier, R.W., Wilson, B.B., 2000. An Atlas of the Kansas High Plains Aquifer, Educational Series 14. Kansas Geological Survey. The University of Kansas, Lawrence, Kansas.

Staggenborg, S.A., Dhuyvetter, K.C., Gordon, W.B., 2008. Grain sorghum and corn comparisons: Yield, economic, and environmental responses. Agron. J. 100, 1600–1604. https://doi.org/10.2134/agronj2008.0129.

Steward, D.R., Allen, A.J., 2016. Peak groundwater depletion in the High Plains Aquifer, projections from 1930 to 2110. Agric. Water Manag. 170. https://doi.org/10.1016/j.agwat.2015.10.003.

Steward, D.R., Bruss, P.J., Yang, X., Staggenborg, S.A., Welch, S.M., Apley, M.D., 2013. Tapping unsustainable groundwater stores for agricultural production in the High Plains Aquifer of Kansas, projections to 2110. Proc. Natl. Acad. Sci. USA 110. https://doi.org/10.1073/pnas.1220351110.

Steward, D.R., Peterson, J.M., Yang, X., Bulatewicz, T., Herrera-Rodriguez, M., Mao, D., Hendricks, N., 2009. Groundwater economics: An object-oriented foundation for integrated studies of irrigated agricultural systems. Water Resour. Res. 45. https://doi.org/10.1029/2008WR007149.

Stoecker, A.L., Seidmann, A., Lloyd, G.S., 1985. A linear dynamic programming approach to irrigation system management with depleting groundwater. Manag. Sci. 31, 422–434. https://doi.org/10.1287/mnsc.31.4.422.

Theis, C.V., 1935. The relation between the lowering of the piezometric surface and the rate and duration of discharge of a well using ground-water storage. Eos Trans. Am. Geophys. Union. 16, 519–524. https://doi.org/10.1029/TR016i002p00519.

Tiemann, L.K., Grandy, A.S., 2015. Mechanisms of soil carbon accrual and storage in bioenergy cropping systems. GCB Bioenergy 7, 161–174. https://doi.org/10.1111/gcbb.12126.

Trout, T.J., DeJonge, K.C., 2017. Water productivity of maize in the US high plains. Irrig. Sci. 35, 251–266. https://doi.org/10.1007/s00271-017-0540-1.

U.S. Energy Information Administration, 2024. Monthly Energy Review: Renewable Energy. February 2024. U.S. Department of Energy, Washington, DC. https://www.eia.gov/totalenergy/data/monthly/. February 2024.

USDA Economic Research Service, 2023. Irrigated Agriculture Is Concentrated in Relatively Few Areas of the United States. U.S. Department of Agriculture. https://www.ers.usda.gov/data-products/chart-gallery/chart-detail?chartId=58346. accessed 15 June 2025.

USDA National Agricultural Statistics Service, 2022. Census of Agriculture. https://www.nass.usda.gov/Publications/AgCensus/2022/ (accessed 15 June 2025).

USDA National Agricultural Statistics Service, 2024a. Cropland Data Layer. https://nassgeodata.gmu.edu/CropScape/.

USDA National Agricultural Statistics Service, 2024b. QuickStats Database: Crop yield data (2000-2018). Available at: https://quickstats.nass.usda.gov/ (accessed 15 June 2025).

USDA National Agricultural Statistics Service, 2024c. QuickStats Database: Crop prices and land rent (2013-2018). Available at: https://quickstats.nass.usda.gov/ (accessed 15 June 2025).

Vaux, H., 2011. Groundwater under stress: the importance of management. Environ. Earth Sci. 62, 19–23. https://doi.org/10.1007/s12665-010-0490-x.

Wallander, S., Aillery, M., Hellerstein, D., Hand, M., 2013. The Role of Conservation Programs in Drought Risk Adaptation.

Warren, J., Stoecker, A., Gatlin, J., Ramaswamy, K., Jones, R., Campiche, J., Paul, A., 2015. Optimizing the economic value water from Ogallala Aquifer used for irrigation. Okla. Water Resour. Cent. Stillwater Okla.

Wheeler, E., Golden, B., Johnson, J., Peterson, J., 2008. Economic efficiency of short-term versus long-term water rights buyouts. J. Agric. Appl. Econ. 40, 493–501. https://doi.org/10.1017/S1074070800023786.

Xie, Y., Gibbs, H.K., Lark, T.J., 2021. Landsat-based irrigation dataset (LANID): 30 m resolution maps of irrigation distribution, frequency, and change for the US, 1997-2017. Earth Syst. Sci. Data 13, 5689–5710. https://doi.org/10.5194/essd-13-5689-2021.

Young, R., Foster, T., Mieno, T., Valocchi, A., Brozović, N., 2021. Hydrologic-economic trade-offs in groundwater allocation policy design. Water Resour. Res. 57, e2020WR027941. https://doi.org/10.1029/2020WR027941.